

We thank the referees for their reviews. To facilitate the review process we have copied the reviewer comments in black text. Our responses are in regular blue font. We have responded to all the referee comments and made alterations to our paper (in bold text).

### **Anonymous Referee #1**

R1.0) This paper describes a modeling study aimed at understanding the relative role of different oxidants within “oxidation flow reactors” (OFRs), flow tubes that have recently seen a lot of attention in atmospheric chemistry as a way to rapidly expose organic species to the equivalent of hours to days of oxidation. The aim is to assess the extent to which non-tropospherically-relevant oxidation processes may occur within such reactors. The authors conclude that under the vast majority of conditions (especially in field studies), OH oxidation dominates over photolysis and initiation by other oxidants, pointing to its utility as an “OH-only” aging reactor.

R1.1) The chemical modeling is quite comprehensive, and the paper makes a very compelling case for the dominance of OH oxidation for the range of compounds examined. However, this range is also the main limitation of the study – the modeling largely covers lightly-oxidized species only. Hydrocarbons and mono-substituted oxygenates are explored fairly well, but the more oxidized, multifunctional species are not. Such species are significant for two reasons: (1) they are major players in chemistry related to multi-day oxidation processes and secondary organic aerosol (SOA) formation, the main targets of OFR studies, and (2) such multifunctional species are likely to photolyze much more readily than the less-oxidized compounds covered in this work. Thus this work really only shows that OH dominates over photolysis for the oxidation of hydrocarbons and first-generation oxidation products, but not necessarily for later-generation species. As a result, many of the strongly-worded conclusions in the manuscript, involving the dominance of OH reactions, simply might not be valid after 1-2 generations of oxidation. Specific concerns related to these multifunctional species are:

- R1.1.1) A few di-functional species are included (some C2-C4 species), but nothing like the sort of multi-substituted molecules that models predict to be in SOA (e.g., Johnson et al., *Env. Chem* 1, 150-165, 2004; Camredon et al., *Atmos. Chem. Phys.* 7, 5599– 5610, 2007) or have been recently measured using CIMS techniques. In fact even the O/C ratios of aerosol generated within the PAM (e.g., Ortega, Lambe papers) would suggest one functional group for each 1-3 carbon atoms. For these molecules, there is a good chance that several of them will be located on adjacent carbon atoms, potentially leading to conjugated systems with much higher cross sections than from any of the individual functional groups. (The C-C bonds in between these functional groups may also be weakened, increasing dissociation quantum yields.)

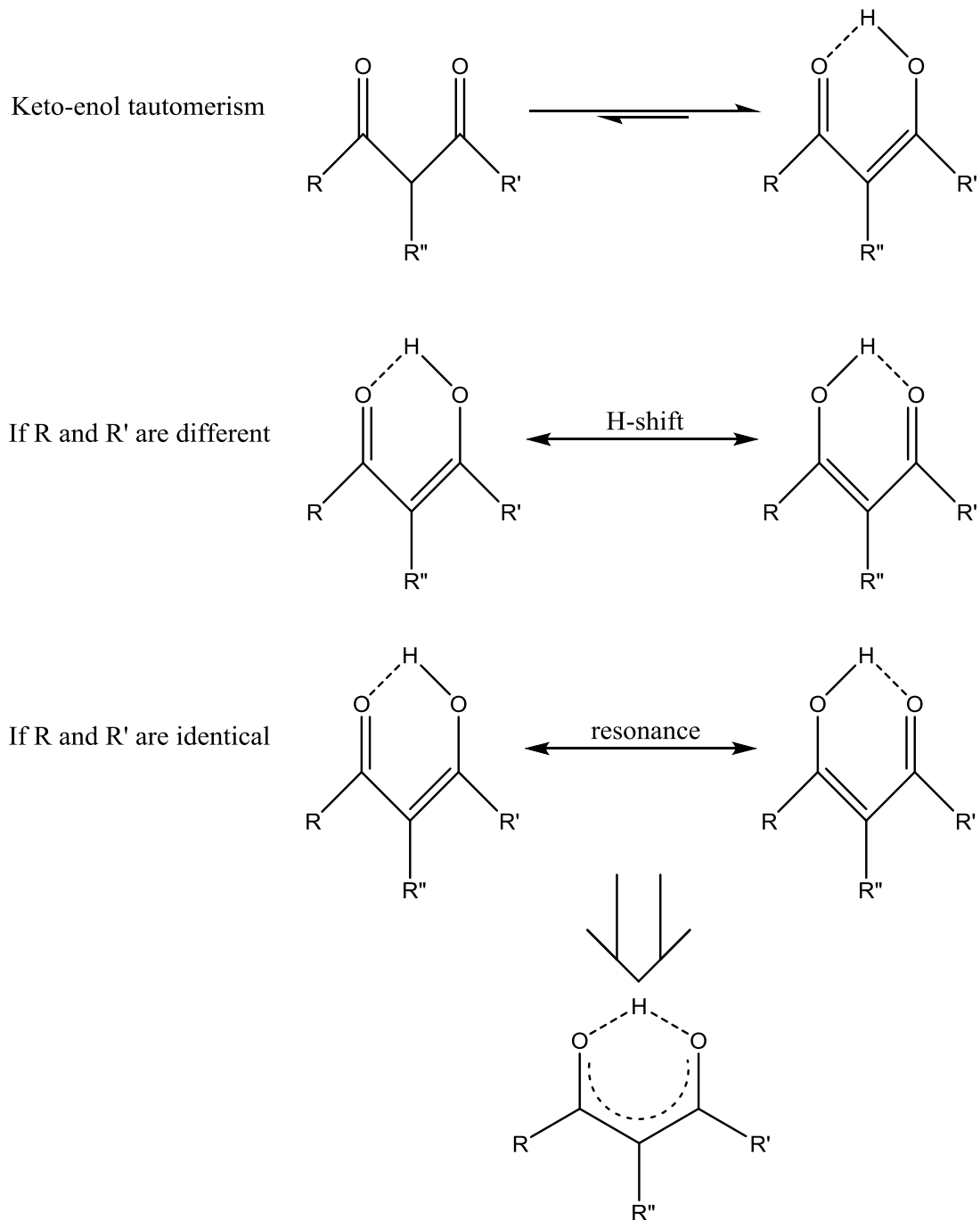
We agree that conjugated or multifunctional molecules may have higher absorption cross-sections. However, we believe that species with high absorptivity due to multiple functional groups are also likely to have low photolysis quantum yields, and hence that these species may photolyze at moderate rates, even if they absorb light efficiently. In addition, conjugated species

also have high reactivity toward OH, resulting in an estimated relative importance of their photolysis that is not higher than for the species discussed in the ACPD paper. To discuss these two types of species (multifunctional and conjugated) in detail, we have modified the text at P23555/L8 (this and all other page / line numbers refer to the ACPD version) to read:

**“Unsaturated carbonyls may have much higher absorption cross-sections if their C=C bonds are conjugated with carbonyls. However, according to our following analysis, conjugated unsaturated carbonyl compounds do not often cause problems of non-tropospheric photolysis at 254 nm. Carbonyls have  $\pi$ - $\pi^*$  and  $n$ - $\pi^*$  transitions. The former corresponds to high cross-section (typically  $>10^{-18}$  cm<sup>2</sup>) and typically occurs around or below 200 nm. The latter is forbidden, and thus has weak absorption (cross-section on the order of  $10^{-19}$  cm<sup>2</sup> or lower), and typically occurs around or above 300 nm (Turro et al., 2009). Conjugation usually does not substantially enhance the absorption of  $n$ - $\pi^*$  transition, but it does for  $\pi$ - $\pi^*$  transitions (Turro et al., 2009). As a result, through conjugation, the only reason why cross-sections of carbonyls at 254 nm may be elevated above  $10^{-18}$  cm<sup>2</sup> is the red-shift of the maximum absorption wavelength of their  $\pi$ - $\pi^*$  transitions due to conjugation. According to Woodward’s rules (Pretsch et al., 2009) and available cross-section data of  $\alpha,\beta$ -unsaturated carbonyls in Keller-Rudek et al. (2015), a conjugation of at least 3–4 double bonds is required for the excitation at 254 nm to dominantly correspond to  $\pi$ - $\pi^*$  transition. Conjugated oxidation intermediates containing at least 3–4 double bonds including C=C bond(s) are virtually impossible to form from aliphatic hydrocarbon oxidation in OFRs. Nevertheless, such intermediates may form via ring-opening pathways of aromatic oxidation (Calvert et al., 2002; Atkinson and Arey, 2003; Strollo and Ziemann, 2013). E,E-2,4-hexadienedial may be regarded as an example of this type of intermediates. Even under assumption of a unity quantum yield, its fraction of photolysis at 254 nm is not much higher than that of aromatic precursors (Fig. 2). Therefore, 254 nm photolysis of conjugated intermediates should not be problematic as long as safer experimental conditions are adopted.**

To our knowledge, the only exception that has strong absorption at 254 nm due to conjugation with  $<2$  double bonds are  $\beta$ -diketones, which may be formed in aliphatic hydrocarbon oxidation, particularly that of long-chain alkanes (Ziemann and Atkinson, 2012). The peculiarity of  $\beta$ -diketones is that their enol form may have a highly conjugated ring structure due to very strong resonance (Scheme S1), and hence cross-sections of the order of  $10^{-17}$  cm<sup>2</sup> at 254 nm (Messaadia et al., 2015). However, even under the assumption of unity quantum yield, the fractional contribution of 254 nm photolysis of acetylacetone (representative of  $\beta$ -diketones) is only slightly larger than for aromatic VOCs (Fig. 2), since its enol form also contains a C=C bond leading to very high reactivity toward OH. Furthermore, we argue that the actual probability that a concrete structural change (in number and type of functional groups, O/C ratio, average C oxidation state etc.) of  $\beta$ -diketones resulting from photoexcitation at 254 nm may be low. As their excitation at 254 nm corresponds to  $\pi$ - $\pi^*$  transition, their rigid ring structure likely hinders cyclic structural change at the 1<sup>st</sup> singlet excited state ( $S_1(\pi,\pi^*)$ ) while the biradical structure of the 1<sup>st</sup> triplet state ( $T_1(\pi,\pi^*)$ ) may favor H-shift between two O

atoms, which ends up with the same/similar structure than prior to the H-shift (Scheme S1). Also, the excitation of  $\beta$ -diketones at 254 nm may also lead to charge transfer complex formation via direct excitation and/or radiationless transition from a local excited state (Phillips and Smith, 2015), which is likely to result in low quantum yields, as discussed in detail below.



**Scheme S1.** Keto-enol tautomerism of  $\beta$ -diketone, and H-shift between O atoms or resonance of the enol form. Note that the tautomerism is generally favorable toward the enol form (Burdett and Rogers, 1964) and that the enol form, particularly its resonance, results in an extensive conjugated ring structure, which may have high absorptivity.

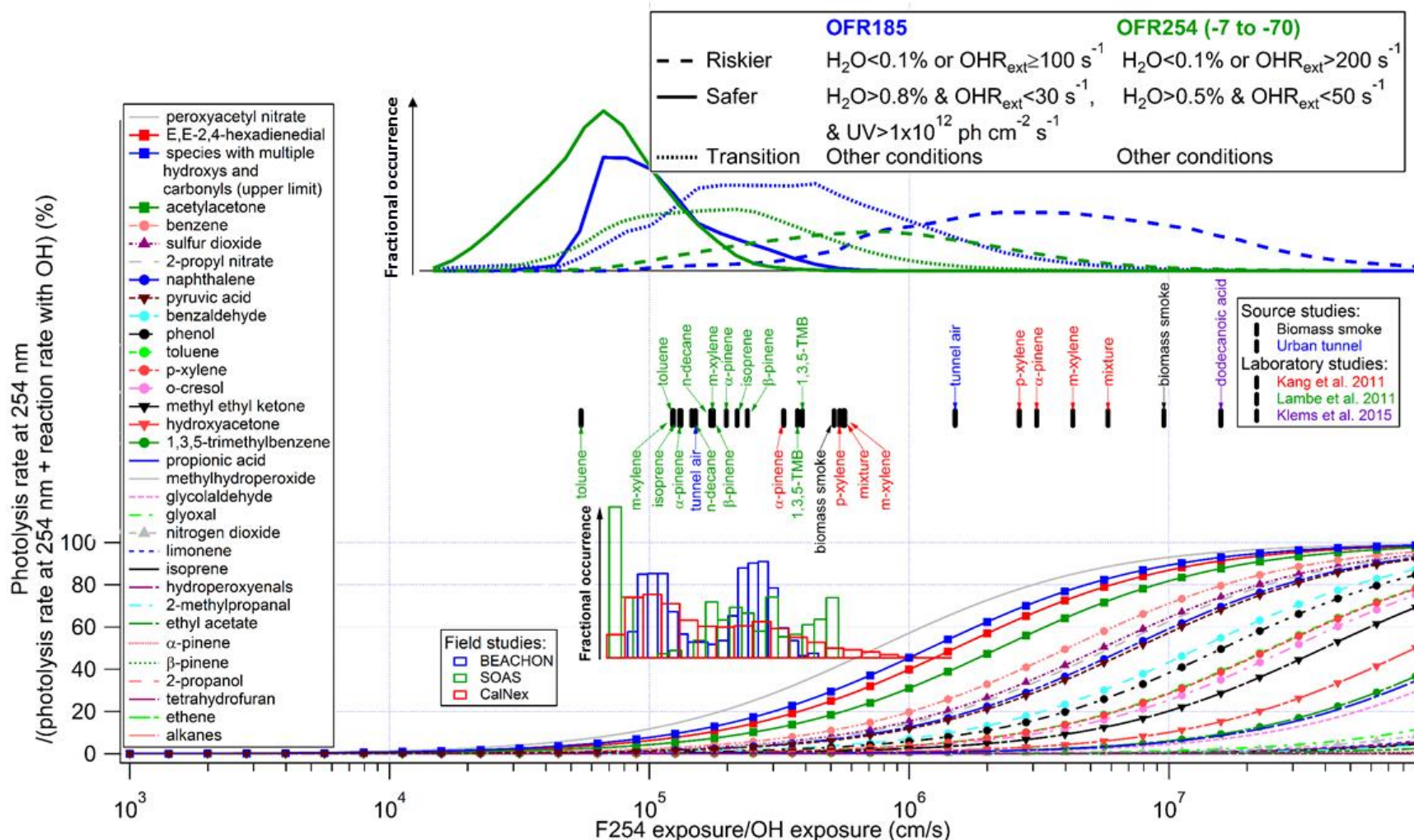


Figure 1. Same format as Fig. 1, but for the fractional importance of the photolysis rate at 254 nm vs. the reaction rate with OH as a function of the ratio of exposure to 254 nm (F254) and OH. The modeled frequency distributions of ratios of 254 nm photon exposure to OH exposure under riskier, safer, and transition conditions for OcFR185 and OFR254 (-7 to -70) are also shown. The curves of saturated carbonyl compounds and possible highly absorbing oxidation intermediates are highlighted by downward triangles and squares, respectively. The insets show histograms of model-estimated F254/OH exposures for three field studies where OFR185 was used to process ambient air. In addition to source studies of biomass

smoke (FLAME-3) and urban tunnel (Tkacik et al., 2014), F254 exposure/OH exposure ratios in two laboratory studies (Kang et al., 2011; Lambe et al., 2011) are shown in the upper inset. Colored tags indicate species used in the laboratory experiments. The lower and upper limits of F254 exposure/OH exposure ratios in the experiments with a certain source in a certain study are denoted by tags below and above the markers, respectively.

In addition to conjugated species, Phillips and Smith (2014, 2015) reported a new type of highly absorbing species that may be formed from VOC oxidation. Although their studies were conducted in the condensed phase, it is likely that the main conclusions of these studies are generally transferable to the gas-phase conditions, since no long-range interactions, which do not exist in normal gases, were involved in these studies. Phillips and Smith (2014, 2015) investigated the photoabsorption enhancement of multifunctional oxygenated species in SOA and found that the high absorptivity of these species can largely be explained by transitions toward the electronic states of charge transfer complex formed between hydroxyl groups (donor) and neighboring carbonyl groups (acceptor). They also pointed out that charge transfer complexes of this kind have a continuum of states whose energy levels range from that of local excited states (radiative transition wavelength <300 nm) to very low levels (radiative transition wavelength >600 nm). The latter are insufficient to cause common photochemical reactions. Relaxation through a continuum of states is usually ultrafast according to Fermi's golden rule (Turro et al., 2009), likely leading to low quantum yields of chemical reactions. The low quantum yields may be seen even from species with only one hydroxyl and one carbonyl: the photolysis of 3-hydroxy-3-methyl-2-butanone and 4-hydroxy-2-butanone at wavelengths down to 270 nm has quantum yields around only 0.1 (Bouzidi et al., 2014, 2015). Although measurements of photolysis quantum yield for multifunctional species are challenging and rare, it is reasonable to expect even lower quantum yields for larger and/or highly substituted (by hydroxyl and carbonyl) species, since larger species have more degrees of freedom for relaxation of excited molecules, and more and/or larger complex sites generally lead to more efficient relaxation through a continuum of states, in accordance with common photophysical sense (Sharpless and Blough, 2014). Therefore, even though species with a number of hydroxyls and carbonyls are formed in VOC oxidation and absorb >1 order of magnitude more efficiently at 254 nm than mono- and difunctional species, they may still have low effective photolysis rates because of low quantum yields.

For this type of species, we estimate an upper limit of the fractional importance of their photolysis at 254 nm. Molar absorption coefficients of charge transfer transitions of organic molecules are usually  $\sim 10^3$ – $1 \times 10^4$  L mol<sup>-1</sup> cm<sup>-1</sup>, i.e., cross-sections of  $\sim 3.9 \times 10^{-18}$ – $3.9 \times 10^{-17}$  cm<sup>2</sup> (Foster, 1969). Based on that, it is reasonable to estimate an upper limit of absorption cross-sections of charge transfer transitions of  $5 \times 10^{-17}$  cm<sup>2</sup>. On the other hand, photolysis quantum yields of multifunctional species are unlikely to be larger than that of species with only one carbonyl and one hydroxyl, i.e.,  $\sim 0.1$  (see discussion above). We thus take 0.1 as an upper limit of photolysis quantum yields. Besides,  $6 \times 10^{-12}$  cm<sup>3</sup> molecule<sup>-1</sup> s<sup>-1</sup> can be a conservative estimate of rate constants of multifunctional oxygenated species with OH, as it is roughly an average value for ketones (Atkinson and Arey, 2003), and the enhancement of H-abstraction by hydroxyl groups (Kwok and Atkinson, 1995; Ziemann and Atkinson, 2012) and the fast abstraction of aldehydic H atoms (Atkinson and Arey, 2003) are completely neglected. With the three estimates combined, the estimated maximum fractional contribution from photolysis at 254 nm to

the fate of multifunctional species is close to that of E,E-2,4-hexadienedial and acetylacetone.

The problem of photolysis of oxidation intermediates at 185 nm is unlikely to be worse than at 254 nm. According to available UV spectra of carbonyl compounds in Keller-Rudek et al. (2015), 185 nm is almost always located within the  $\pi$ - $\pi^*$  transition band, whose maximum cross-section is on the order of  $10^{-17}$  cm<sup>2</sup>. Even if all types of radiative transitions at normal radiation intensity are considered, an approximate upper limit of absorption cross-sections is  $\sim 10^{-16}$  cm<sup>2</sup> (Evans et al., 2013). However, UV intensity at 185 nm in the OFR185 mode is  $\sim 100$  times lower than that at 254 nm (Li et al., 2015). The photolysis rate of oxidation intermediates at 185 nm should thus be generally smaller than at 254 nm.

Therefore, in summary, photolysis of oxidation intermediates are, to our knowledge, conservatively estimated to be of limited importance relative to their reactions with OH, as long as the experimental conditions are in the safer range. Although studies on photolysis quantum yields of oxidation intermediates are very sparse, we reason, based on the existing studies on this topic and common photophysical and photochemical rules, that the photolysis quantum yields of these species may be lower than the values assumed in this study (e.g., 1 for E,E-2,4-hexadienedial and acetylacetone and 0.1 for multifunctional species). As a result, actual rates and relative importance of photolysis might be significantly smaller than the upper limits estimated in our study.”

We have also inserted the following paragraph in P23554/L7:

“Oxidation intermediates may also photolyze at 185 nm. However, their photolysis is unlikely to be significant when OFR is not operated at low H<sub>2</sub>O and/or high OHR<sub>ext</sub>. To clarify this issue, a detailed discussion about the photolysis of oxidation intermediates at 254 nm is required as a premise. We thus discuss oxidation intermediate photolysis at both 185 and 254 nm in Section 3.1.3.”

We have also modified the text in P23555/L23 to read:

“Note that photolysis of oxidation intermediates also needs to be taken into account. If multifunctional species,  $\beta$ -diketones, and extensively conjugated species are photolyzed as shown in Fig. 2, these photolyses would be significant in some previous source and laboratory studies examined here, as they were conducted at relatively low H<sub>2</sub>O and/or high OHR<sub>ext</sub>. To our knowledge, none of these studies reported a significant photolysis of oxidation intermediates. Klems et al. (2015) attributed large amounts of fragmentation products detected in their OFR experiments with dodecanoic acid to photolysis of peroxy radicals. However, these products may also be at least partially accounted for by photolysis of carbonyls leading to carbon-chain cleavage via Norrish reactions (Laue and Plagens, 2005). The OFR used by Klems et al. (2015) has a different design from the PAM, which is regarded as the base design in this study. Their reactor employs a light source

stronger than the PAM's highest lamp setting, with UV at 254 nm estimated to be  $\sim 3 \times 10^{16}$  photons  $\text{cm}^{-2} \text{s}^{-1}$  ( $\sim 4$  times the value at the highest lamp setting of the PAM OFR) based on the lamp power and the reactor geometry. Such high UV may even result in significant photolysis of saturated carbonyl intermediates, which are very likely formed in the oxidation of long-chain alkane-like dodecanoic acid."

We also modify the text P23566/L7 to read:

"In laboratory experiments, running OFRs under safer conditions ensures a minor contribution of non-tropospheric photolysis, based on the current knowledge of oxidation intermediate photolysis (Fig. 2). This also reduces the relative contribution of ozonolysis to VOC fate. However, when more information becomes available about photolysis quantum yields of oxidation intermediates (vs. the upper limits assumed here), there may be additional flexibility to include ozonolysis while excluding non-tropospheric VOC consumption. As the precursor composition is usually relatively simple in laboratory experiments, it is sufficient to ensure the insignificance of non-tropospheric consumption of only the precursor(s) and possible intermediates (usually oxygenated species), rather than for a large variety of VOC precursors and intermediates. For example, in the case of quantum yields significantly lower than used in the present work, we may perform OFR254-70 experiments with a large amount of biogenics at medium  $\text{H}_2\text{O}$  and UV. In this case, a tropospheric  $\text{O}_{3\text{exp}}/\text{OH}_{\text{exp}}$  ratio can be obtained without major side effects, because the fractional contribution of photolysis of possible intermediates is still minor due to low quantum yields. On the other hand, OFR experiments with some anthropogenic VOCs, such as alkanes, can just be conducted at high  $\text{H}_2\text{O}$  and low  $\text{OHR}_{\text{ext}}$  to avoid the contribution of all non-OH reactants, since ozonolysis of alkanes is negligible even at a tropospheric  $\text{O}_{3\text{exp}}/\text{OH}_{\text{exp}}$ ."

- R1.1.2) Some broad generalizations are made about the photolysis of nitrates and peroxides (e.g., page 23555 line 5). However only one nitrate (with 3 carbon atoms) and one peroxide (with 1 carbon atom) were actually studied. (PAN has a peroxy group - given it has no C-O-N bonding moiety, it is not truly a nitrate - and hydroperoxyenal cross sections have never actually been measured, but rather only estimated based on cross sections of similar but nonperoxidic species.) Larger or more functionalized species may well exhibit very different photolytic behavior.

We already stated in the ACPD manuscript that "we include one or two representative species for a category of species with certain functional group(s)" in Section S1. This does not mean that we made broad generalizations based on the data of only one species but that we selected for graphical display 1–2 species whose data are representative enough for the category. In fact, we did include the photolysis of 4 additional nitrates (methyl nitrate, ethyl nitrate, 1-propyl nitrate, and 1-butyl nitrate) in Fig. 6. We did also find UV spectra of more or larger nitrates (e.g., 2-butyl nitrate, 2-pentyl nitrate, 3-pentyl nitrate, cyclopentyl nitrate, 3-methyl-1-butyl nitrate, and 1-pentyl nitrate) in Keller-Rudek et al. (2015), but did not include them in Fig. 6 to avoid clutter,

since the UV-Vis spectra of most simple organic nitrates, with the nitrate group dominating the absorption, are very similar.

We agree that PAN is not a nitrate, and have replaced “nitrate(s)” with “nitrate(s) and peroxyxynitrate(s)” throughout the manuscript whenever necessary.

We agree that the proxy of hydroperoxyenals used in the ACPD version (E-2-hexanal) was nonperoxidic. The absorption of hydroperoxyenals at 254 nm should have the contribution from hydroperoxy group (cross-section of methylhydroperoxide at 254 nm:  $3.23 \times 10^{-20}$  cm<sup>2</sup>), which is likely larger than the cross-section of the nonperoxidic proxy at 254 nm ( $\sim 2 \times 10^{-21}$  cm<sup>2</sup>). We thus replaced the 254 nm cross-section of hydroperoxyenals used in the ACPD version with that of methylhydroperoxide. We made corresponding changes to Figs. 2 and S2 and Table S1.

To clarify why the data of 254 nm cross-section of hydroperoxyenals in Table S1 is used, we also added the following note to Table S1:

**“\*5: value of a proxy, methylhydroperoxide, is used as the proxy used in Wolfe et al. (2012), E-2-hexanal, does not contain a hydroperoxy group and hence has little absorption at 254 nm.”**

However, we argue that the absorption of hydroperoxy groups may be more due to themselves than to their interactions with adjacent functional groups. It is unlikely that as dramatic an absorption enhancement could occur between a carbonyl group and a hydroperoxy group as between a carbonyl group and a hydroxyl group. The charge transfer from hydroxyl to carbonyl should take place between the former’s HOMO (highest occupied molecular orbital), n-orbital (non-bonding), and the latter’s possible positive hole, i.e., the orbital from which an electron of the carbonyl is excited by a photon. These two orbitals should be of close energy level so that their interaction for charge transfer can be significant (Carey and Sundberg, 2007). However, the HOMO of a hydroperoxy group is an anti-bonding  $\pi^*$ -orbital, whose energy is much higher than that of non-bonding n-orbital of a hydroxyl group. As a consequence, a significant reorganization of their geometric configuration might be required for the interaction between the donor and acceptor orbitals to be maximized (Turro et al., 2009). This requirement might suppress charge transfer between carbonyl and hydroperoxy.

For larger and more functionalized species, see response to R1.1.1.

- R1.1.3) The choices for SOA components (Table S6) are non-obvious. I understand that due to the lack of data, surrogate compounds need to be used. But as described above, SOA molecules will mostly have more than 1-2 functional groups, and therefore may absorb light much more strongly than any of the species listed. There may well also be intermolecular interactions that affect absorption further. The values given should thus be treated as strict lower limits, not averages. In fact, recent measurements find the cross section of  $\alpha$ -pinene+O<sub>3</sub> SOA to be about  $3 \times 10^{-19}$  cm<sup>2</sup> (Wong et al., JPCA 119,

4309–4316, 2015), ~1 order of magnitude higher than any of the (non-aromatic) surrogates used in this study.

We agree that real SOA samples have higher absorption cross-section than the non-aromatic surrogates used in the ACPD manuscript, according to Wong et al. (2015), as well as the references suggested by Referee #2 (see R2.7). We have included these data into Table S7 (Table S6 in the ACPD paper) and Fig. 8.

Indeed, there may also be condensed-phase intermolecular interactions affecting SOA absorption, similar to intramolecular charge transfer in the gas phase discussed above. However, these intermolecular interactions may also lead to low photolysis quantum yields, for the same reason discussed above (Phillips and Smith, 2014, 2015). Moreover, the condensed phase may provide more efficient pathways facilitating the relaxation of excited states than the gas phase, because of fast interactions with the surrounding molecules (Turro et al., 2009). In summary, SOA absorption can be significantly enhanced, but its photolysis rate may not, because of low quantum yields resulting from efficient relaxation.

In addition, we have modified the paragraph in P23563/L6 to read:

**“Recently, photolysis in the UV range has been found to be a potentially significant sink of some types SOA in the troposphere (Updyke et al., 2012; Lambe et al., 2013; Liu et al., 2013, 2015; Hodzic et al., 2015; Wong et al., 2015; Romonosky et al., 2016). It is necessary to also investigate SOA photolysis in OFRs, as photons used in OFRs are highly energetic and non-tropospheric. UV extinction due to aerosol optical scattering and in-particle absorption under OFR conditions is generally negligible (Hodzic et al., 2015). For simplicity, we estimate photodegradation ratios of various SOA component surrogates as well as several SOA samples whose absorptivity was measured in previous studies (Updyke et al., 2012; Lambe et al., 2013; Liu et al., 2013; Romonosky et al., 2016) (Fig. 8) under the assumption of unity quantum yield to obtain upper limits of photodegradation ratios, and also under the assumption of lower (0.1 and 0.01) quantum yields.”**

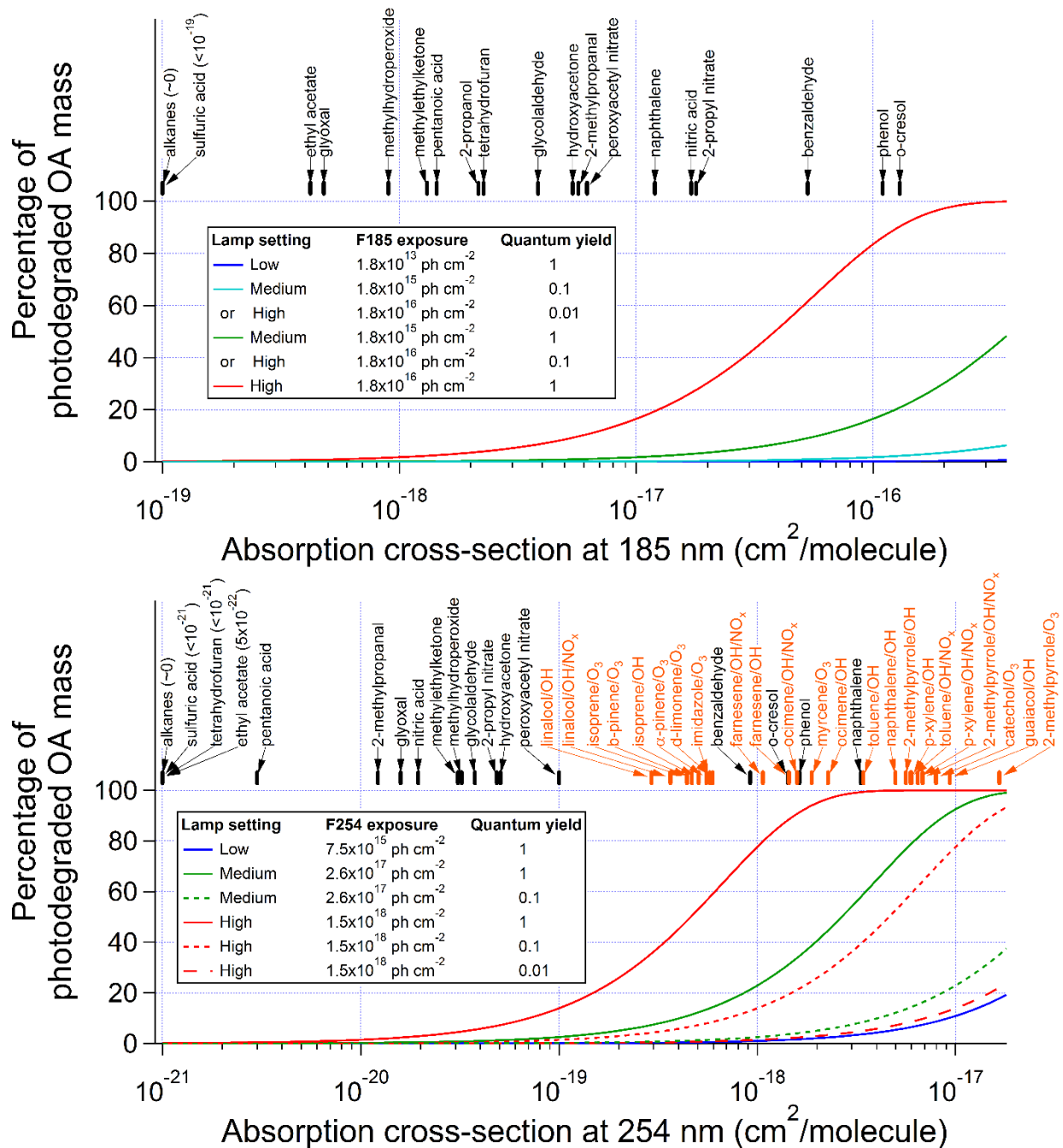


**Figure 2. Percentage of SOA photodegradation at (upper panel) 185 and (lower panel) 254 nm at different UV levels as a function of absorption cross-section under the assumptions of quantum yields of 1, 0.1, and 0.01. Absorption cross-sections of some SOA component surrogates (black tag) and SOA samples (orange tag; calculated from data in Lambe et al. (2013) and Romonosky et al. (2015a)) are also shown.**

We have also modified the following text in P23564/L13 to read:

“Wong et al. (2015) conducted  $\alpha$ -pinene-derived SOA photolysis experiments in a chamber under UVB irradiation (down to 284 nm). They observed at 85% RH ~30% SOA photolyzed after >30 min irradiation and a photolysis quantum yield of ~1 during the first 10 min. However, in OFRs such a high SOA photodegradation percentage would not occur, since Wong et al. (2015)’s experiments had a high photon flux ( $\sim 4 \times 10^{15}$  photons  $\text{cm}^{-2} \text{s}^{-1}$ ) and a long irradiation time, and hence a photon flux exposure that is ~5 times that at the highest lamp setting in the OFRs modeled in our work. According to the measurements of Wong et al. (2015), a photolysis fraction of ~6% would be expected for this type of SOA in our OFRs under the highest UV flux, with lower percentages at lower UV settings. In addition, the approximate unity quantum yield observed in Wong et al. (2015) may be due to (hydro)peroxides in  $\alpha$ -pinene-derived SOA, since peroxides have high photolysis quantum yields (Goldstein et al., 2007; Epstein et al., 2012), while other functional groups (i.e., mainly hydroxyl and carbonyl) in oxygenated species in SOA are unlikely to have for reasons discussed below.

Note that a simple addition of absorptivities of different functional groups may not explain SOA absorptivity (Phillips and Smith, 2015). According to the absorption data of SOA samples from Lambe et al. (2013) and Romonosky et al. (2015a), real SOA absorbs ~1–3 orders of magnitude more than non-aromatic component surrogate species shown in Fig. 8 at 254 nm. As discussed for multifunctional oxidation intermediates (with carbonyls and hydroxyls), SOA absorption enhancement may be largely due to transitions of charge transfer complexes formed between carbonyls and hydroxyls in multifunctional oxygenated SOA components (Phillips and Smith, 2014, 2015). These complexes between carbonyls and hydroxyls also have continua of states likely leading to ultrafast relaxation and hence low photolysis quantum yields. Charge transfer transitions have been extensively shown in measurements (Alif et al., 1991; Gao and Zepp, 1998; Johannessen and Miller, 2001; O’Sullivan et al., 2005; Zhang et al., 2006; Osburn et al., 2009; Sharpless and Blough, 2014) to have very low quantum yields in the condensed phase. Sharpless and Blough (2014) compiled quantum yields of various products of humic-like matter photolysis down to 280 nm. No quantum yields except those of the product  $^1\text{O}_2$ , which is generally unimportant for OFRs (see Section 3.1.6), are higher than 0.01. If the photolysis quantum yields of the SOA samples in Fig. 8 at 254 nm are no more than 0.01, no SOA samples will be photolyzed by 20% even at the highest OFR lamp setting, and photolysis of most SOA samples at 254 nm will be minor or negligible in OFRs. Thus, to our current knowledge, lack of solid information on quantum yields of SOA components with multiple carbonyls and hydroxyls at 254 nm prevents a clear assessment of SOA photolysis in OFRs at the medium and high UV. On the other hand, direct measurements are desirable for this issue and caution should still be exercised for OFR experiments at relatively high UV.

SOA photolysis at 185 nm may be lower compared to that at 254 nm. SOA absorptivity data at 185 nm are not available. According to SOA mass-specific absorption cross-section (MAC) data between 250 and 300 nm in Romonosky et al. (2015a), there is a linear relationship between the logarithm of MAC and wavelength for most SOA samples: MAC

increases by a factor of ~3 per 50 nm decrease in wavelength. We thus extrapolate this relationship to 185 nm, where MAC is estimated to be ~3.5 times higher than that at 254 nm. However, the UV flux at 185 nm in our OFR is ~100 times lower than at 254 nm.

Based on the discussion above, the SOA photodegradation ratio of ~30% in Wong et al. (2015)'s non-OFR setup may be explained.  $\alpha$ -pinene-derived SOA has ~20–50% weight fraction of peroxides (Docherty et al., 2005; Epstein et al., 2014), which may undergo photolysis in SOA to convert into carbonyls (and hydroxyls) (Epstein et al., 2014). We speculate that after the formation of carbonyls from peroxides, SOA materials cannot proceed significantly further with photolysis as discussed for charge transfer between carbonyl and hydroxyl above. In the experiments of Wong et al. (2015), as well as Epstein et al. (2014), effective photolysis rate constants/quantum yields decreased as SOA photolysis proceeded. Photolysis rates were substantially reduced after a ~30% mass loss due to photolysis in Wong et al. (2015)'s experiments. This mass loss ratio is consistent with the mass percentage of peroxides in  $\alpha$ -pinene-derived SOA. Again, we note that, according to the extrapolation from Wong et al. (2015)'s results, the mass loss percentage expected in our OFR under the highest UV flux is ~6% for  $\alpha$ -pinene-derived SOA. This value is much lower than that shown in Fig. 8 under the assumption of unity quantum yield (~40%) because of a substantially decreasing quantum yield in the real photolysis experiments. Therefore, in OFRs, even if (hydro)peroxides in SOA may be photolyzed in appreciable amounts, SOA mass is unlikely to be largely destroyed by photons in OFRs, as (hydro)peroxides may convert into carbonyls and hydroxyls, which may substantially lower subsequent photolysis quantum yields.

According to the discussion above, measurements of quantum yields and/or products of SOA photolysis are highly desirable, especially for the photolysis of SOA containing dominantly carbonyl and hydroxyl groups, as (hydro)peroxides, which are likely to form in OFRs, may convert into hydroxyls and carbonyls. With more data on quantum yields of SOA photolysis, a clearer strategy for including or excluding SOA photolysis in OFRs can be made.

Even though SOA photolysis can be significant in OFRs, it only proceeds to a much lesser extent compared to ambient SOA photolysis. We calculate the numbers of e-fold decay of SOA photolysis in OFR254-70 and the troposphere according to the effective ambient photolysis lifetime of SOA from Romonosky et al. (2015a). Under the condition of 70% RH ( $\text{H}_2\text{O} = 1.4\%$ ) and  $\text{OHR}_{\text{ext}} = 25 \text{ s}^{-1}$  (typical of ambient conditions), SOA samples are estimated to undergo ~0.01–0.5 e-fold photolysis timescales (i.e., ~1–35% OA photolyzed) in OFR254-70 at an equivalent photochemical age of 1 week under the upper limit assumption of unity quantum yields (Table S8). However, in the atmosphere, those samples may proceed with  $10^2$ – $10^4$  e-fold decays of photolysis (i.e., virtually complete destruction) at the same photochemical age, if ambient SOA photolysis quantum yields are assumed to be those of  $\text{H}_2\text{O}_2$  (unity below 400 nm). Even if the quantum yield of acetone (non-zero below 320 nm, see Romonosky et al., 2015a) is taken as a surrogate for SOA, most types of SOA would still be completely or nearly completely photolyzed

under ambient conditions. These results demonstrate that ambient SOA photolysis is likely to be much more important than in OFRs. On the other hand, they also highlight the need for studies of ambient SOA photolysis quantum yields and photolytic aging, as ambient SOA is unlikely to be completely destroyed by photons within only 1 week. Either their quantum yields are much lower than used in this study, or the photolabile groups are destroyed and leave behind others that are not (or less) photolabile during photolytic aging.”

**Table S8. Number of e-fold decays of photolysis and percentage of photolyzed OA of several SOA samples at an equivalent photochemical age of 1 week under atmospheric conditions in Romonosky et al. (2015a) and in OFR254-70 at 70% relative humidity (water vapor mixing ratio of 1.4%) and  $25 \text{ s}^{-1}$  initial  $\text{OHR}_{\text{ext}}$ . Absorption cross-sections at 254 nm and effective ambient photolysis lifetimes of SOA samples are taken from or calculated according to Romonosky et al. (2015a). Ambient photolysis data are obtained assuming quantum yields of SOA samples to be those of  $\text{H}_2\text{O}_2$  or acetone.**

SOA type	Cross-section at 254 nm ( $\text{cm}^2$ )	Effective ambient photolysis lifetime (min)		Number of e-fold decays due to photolysis			Percentage of photolyzed OA at equivalent photochemical age of 1 week		
		Using QY of $\text{H}_2\text{O}_2$	Using QY of acetone	OFR254-70	Ambient using QY of $\text{H}_2\text{O}_2$	Ambient using QY of acetone	OFR254-70	Ambient using QY of $\text{H}_2\text{O}_2$	Ambient using QY of acetone
2-methylpyrrole/ $\text{O}_3$	1.66E-17	1	85	0.461	10080	119	36.9	100	100
guaiacol/OH	9.34E-18	1.7	190	0.259	5929	53	22.8	100	100
catechol/ $\text{O}_3$	7.97E-18	3	260	0.221	3360	39	19.8	100	100
2-methylpyrrole/OH/ $\text{NO}_x$	6.82E-18	1	130	0.189	10080	78	17.2	100	100
p-xylene/OH/ $\text{NO}_x$	6.46E-18	2.5	280	0.179	4032	36	16.4	100	100
p-xylene/OH	5.99E-18	5.5	430	0.166	1833	23	15.3	100	100
toluene/OH/ $\text{NO}_x$	5.93E-18	1.3	190	0.164	7754	53	15.2	100	100
2-methylpyrrole/OH	5.61E-18	2.6	260	0.155	3877	39	14.4	100	100
naphthalene/OH	4.98E-18	0.62	64	0.138	16258	158	12.9	100	100
toluene/OH	3.42E-18	6.2	590	0.095	1626	17	9.1	100	100
ocimene/OH	2.27E-18	25	1700	0.063	403	5.9	6.1	100	99.7
myrcene/ $\text{O}_3$	1.88E-18	58	3800	0.052	174	2.7	5.1	100	93.0
ocimene/OH/ $\text{NO}_x$	1.59E-18	25	1800	0.044	403	5.6	4.3	100	99.6
farnesene/OH	1.44E-18	53	3500	0.040	190	2.9	3.9	100	94.4
farnesene/OH/ $\text{NO}_x$	1.07E-18	47	3400	0.030	214	3.0	2.9	100	94.8
d-limonene/ $\text{O}_3$	5.95E-19	230	7200	0.016	44	1.4	1.6	100	75.3
imidazole/ $\text{O}_3$	5.76E-19	95	4800	0.016	106	2.1	1.6	100	87.8
$\alpha$ -pinene/ $\text{O}_3$	5.54E-19	85	4800	0.015	119	2.1	1.5	100	87.8
isoprene/OH	5.07E-19	410	7600	0.014	25	1.3	1.4	100	73.5
$\beta$ -pinene/ $\text{O}_3$	4.68E-19	90	4000	0.013	112	2.5	1.3	100	92.0

isoprene/O <sub>3</sub>	4.42E-19	88	5400	0.012	115	1.9	1.2	100	84.5
linalool/OH/NO <sub>x</sub>	3.65E-19	100	7700	0.010	101	1.3	1.0	100	73.0
linalool/OH	2.92E-19	160	11000	0.008	63	0.9	0.8	100	60.0

We have accordingly modified the conclusion section in P23567/L22 to read:

**“We assessed the relative significance of the VOC consumption by non-OH reactants to that by OH in OFRs and the troposphere. The only non-tropospheric reaction that can play a major role under OFR conditions is photolysis, especially at 254 nm. The relative importance of photolysis is largest under riskier OFR conditions where OH is low due to low H<sub>2</sub>O and/or high OHR<sub>ext</sub>. Due to lack of quantum yield data, we estimated upper limits of the relative importance of photolysis for the few most susceptible oxidation intermediates, which are comparable to those from aromatic precursors. Reactions of O atoms are not competitive and are actually of lower relative importance (vs. OH) in OFRs than in the troposphere. VOC ozonolysis is much less important than in the troposphere under typical OFR conditions and of similar importance under riskier OFR conditions. Photolysis of SOA in OFRs could be significant at medium and high UV, but only if corresponding quantum yields are high. If SOA photolysis quantum yields are of the order of 0.01 or lower, as measured for many humic-like substances (Sharpless and Blough, 2014), SOA photolysis in OFRs may be minor or negligible under most conditions. Although the reaction fates may be different, numbers of e-fold decays of photolysis for a given OH<sub>exp</sub> are at least an order-of-magnitude lower in the OFRs compared to the troposphere.”**

We have also added the following paragraph to the conclusion section at P23568/L21:

**“The need for systematic measurements of photolysis quantum yields, for both VOC and SOA, and both at actinic wavelengths and at 185 and 254 nm, was highlighted in this study. When quantum yield data become available, photolysis of oxidation precursors, oxidation intermediates, and SOA in OFRs can be much better quantified, its relative importance compared to OH oxidation, ambient photolysis etc. can be better evaluated, and experimental planning might then be able to be less conservative and have more freedom to avoid non-tropospheric photolysis and realize specific experimental objective(s).”**

To make the abstract consistent with the modifications above, we have also modified the text in P23545/L18 to read:

**“Photolysis at non-tropospheric wavelengths (185 and 254 nm) may play a significant (>20%) role in the degradation of some aromatics, as well as some oxidation intermediates, under riskier reactor conditions, if the quantum yields are high. Under riskier conditions, some biogenics can have substantial destructions by O<sub>3</sub>, similarly to the troposphere. Working under low O<sub>2</sub> (volume mixing ratio of 0.002) with the OFR185 mode allows OH to completely dominate over O<sub>3</sub> reactions even for the biogenic species most reactive with O<sub>3</sub>.”**

We have also modified the text in P23545/L26 to read:

**“Photolysis of SOA samples is estimated to be significant (>20%) under the upper limit assumption of unity quantum yield at medium ( $1 \times 10^{13}$  and  $1.5 \times 10^{15}$  photons  $\text{cm}^{-2} \text{s}^{-1}$  at 185 and 254 nm, respectively) or higher UV flux settings. The need for quantum yield measurements of both VOC and SOA photolysis is highlighted in this study.”**

R1.2) The possible fates of the later-generation, multifunctional species therefore need to be examined in more detail in this work. Of course these molecules are highly diverse, and chemical/optical data on them is very sparse. One option would be to extend the quantum chemical calculations to a range of such species, but that would probably be a major project in itself. Instead I would recommend a sensitivity study. If species absorb 254nm or 185nm light at 10x or 100x the cross sections used here, to what extent would photolysis compete with OH? If OH reaction continues to dominate, then the strong conclusions throughout the paper about the importance of OH chemistry still hold; if not, the possibility of photolysis of highly functionalized species needs to be discussed explicitly. (This would suggest an important area of future research, with measurements needed both at these low wavelengths and within the standard actinic window.)

See response to R1.1. Extensively conjugated unsaturated carbonyls formed in aromatic oxidation,  $\beta$ -diketones formed in oxidation of aliphatic moiety, and the extreme case for multifunctional species can be regarded as reasonable upper limits of photolysis relative importance. We thus did not conduct the sensitivity study by simply multiplying cross-sections by 10 or 100 as the Referee suggested.

R1.3) Abstract: an interesting result of this paper is that the model results suggest that under some cases, OH oxidation (relative to other oxidation channels) can actually be more important in the OFR than in the troposphere. This is alluded to in the mention of biogenic species reacting with O<sub>3</sub>, but should probably be said more explicitly in the abstract.

We agree with this comment and have modified the abstract above to clarify this point (see response to R1.1.3).

R.1.4) 23548 line 9: This sentence mentions peroxy-radical photolysis, which has been suggested to be a non-tropospheric reaction path within OFRs. But this is not explored anywhere in the manuscript. Either it needs to be included, or its exclusion from this paper needs to be stated.

We only cover the chemistry of stable species in OFR in this paper and plan to address OFR peroxy radical chemistry in a future paper. Thus, we modify the sentence to P23548/L9 to read:

**“Klems et al. (2015) concluded that photons at 254nm from Hg-lamp emission played an important role in their OFR experiment, especially for downstream chemistry.”**

And we have modified the text in P23548/L12 to read:

**“In this paper, we apply the model in Peng et al. (2015) to systematically investigate whether significant non-tropospheric or non-OH chemistry occurs in OFRs, and what experimental conditions make it more important. Considering the enormous complexity of organic radical (particularly organic peroxy) chemistry, we only examine the non-OH fate of stable species in the present work. The fate of organic radicals should be the subject of future studies.”**

R1.5) 23549/20-21: This section makes reference to the study of non-plug flow conditions in the cited Peng et al. paper. However, I didn't see any such discussion in that paper. Maybe I'm just missing it? Or did the authors use the wrong reference? (Or are they referring to a version that isn't publicly available?)

We apologize for this confusion. We made the statement on P23549/L20-21 based on the additional work for the revision of Peng et al. (2015b). We were hoping that the responses to the referees' comments to Peng et al. (2015b) would be posted much earlier. However, those responses were extensive and their review by coauthors led to their posting after Referee #1's comments to this ACPD paper. Please see these responses at <http://www.atmos-meas-tech-discuss.net/8/C3671/2015/amtd-8-C3671-2015-supplement.pdf>. The final version of Peng et al. (2015b) has been published in AMT and indeed contains an extensive study of the impact of non-plug-flow conditions in OFRs.

R1.6) Figs 1-2 (and S1-S2): The x-axes in these plots, which are not discussed at all in the manuscript, are quite unusual, and probably should be changed. “Exposure” is best defined as “concentration times time”. The x axis is given in units of cm/s; assuming the OH exposure is in the standard units (molecules-s/cm<sup>3</sup>), this would mean the authors are expressing “photon exposure” in molecule/cm<sup>2</sup>, which is very hard to interpret, particularly in terms of an “exposure”. The most intuitive unit to use for photon exposure is photon density times time; this would make the x axis unitless, as is the case for Figs 3-5.

The unit of x-axes in Figs. 1 and 2 (cm s<sup>-1</sup>) can be explained. F185 (F254) exposure is the product of 185 (254) nm photon flux (in photons cm<sup>-2</sup> s<sup>-1</sup>) and time (in s), whose unit is photons cm<sup>-2</sup>, while OH<sub>exp</sub> is in molecules cm<sup>-3</sup> s<sup>-1</sup>. Therefore, F185 (F254) exposure/OH exposure has a unit of cm s<sup>-1</sup>.

Photon density can be obtained as photon flux divided by the speed of light. For instance, a photon flux of 3x10<sup>13</sup> photons cm<sup>-2</sup> s<sup>-1</sup> corresponds to a photon density of 3x10<sup>13</sup> photons cm<sup>-2</sup> s<sup>-1</sup> / (3x10<sup>8</sup> m s<sup>-1</sup>) = 1x10<sup>3</sup> photons cm<sup>-3</sup>. However, photon flux is commonly used for kinetic studies involving light. It is very unusual in our experience to use photon density instead. Therefore, we keep the x-axis unit of Figs. 1 and 2 as it is, and clarify this unit by adding the following text to their caption:

**“F185 (F254) exposure (in photons cm<sup>-2</sup>) is the product of 185 (254) nm photon flux (in photons cm<sup>-2</sup> s<sup>-1</sup>) and time (in s). F185 (F254) exposure / OH exposure is thus in cm s<sup>-1</sup>.”**

R1.7) Figs 2-5: This is a very complicated figure. The laboratory-study parameters might be easier to understand if they were presented as horizontal lines (ranges) rather than two markers with differently-placed labels.

We have worked a lot on these figures and made many different versions, e.g., an alternative version that we experimented with can be seen in Supp. Info. If we present the laboratory-study ranges as horizontal lines, those lines greatly clutter the plots as the space for showing these ranges in Figs. 2–5 is already limited. We thus prefer to keep the format of these figures as it is, except that the horizontal lines (ranges) for OFR are replaced by fractional occurrence distribution of exposure ratios to make them more informative and define “riskier” (“pathological” conditions are now called “riskier” conditions in the revised manuscript) conditions etc. more clearly (see revised Fig. 2 above as an example).

We have replaced the paragraph in P23552/L8 by the following text with new and clearer definitions of the input condition categories to read:

**“In these figures, the relationships of all non-OH reactive species to OH are similar for certain common conditions. We define three types of conditions to help guide experimental design and evaluation in terms of the relative importance of non-OH reactants. Under “riskier conditions” of high/very high  $\text{OHR}_{\text{ext}}$  ( $\geq 100 \text{ s}^{-1}$  in OFR185 and  $> 200 \text{ s}^{-1}$  in OFR254 (-7 to -70)) and/or low  $\text{H}_2\text{O}$  ( $< 0.1\%$ ), non-OH reactions can be significant depending on the species. Conversely, under “safer conditions” with relatively low  $\text{OHR}_{\text{ext}}$  ( $< 30 \text{ s}^{-1}$  in OFR185 and  $< 50 \text{ s}^{-1}$  in OFR254), and high  $\text{H}_2\text{O}$  ( $> 0.8\%$  in OFR185 and  $> 0.5\%$  in OFR254), and moderate or higher UV ( $> 1 \times 10^{12} \text{ photons cm}^{-2} \text{ s}^{-1}$  at 185 nm) in OFR185, reaction with OH is dominant (Figs. 1–5 and S1–5). We denote all other conditions as “transition conditions.” High  $\text{H}_2\text{O}$  and zero/low  $\text{OHR}_{\text{ext}}$  lead to strong OH production and no/weak OH suppression, respectively. Thus, OH is more abundant and dominates species consumption under those conditions. In the case of low  $\text{H}_2\text{O}$  and high  $\text{OHR}_{\text{ext}}$ , OH is generally lower because of less production and more suppression. These conditions increase the relative contribution of non-OH species. UV light intensity is generally less influential on non-OH VOC fate than  $\text{H}_2\text{O}$  and  $\text{OHR}_{\text{ext}}$ , although OH production is nearly proportional to UV (Peng et al., 2015), because the non-OH reactive species also scale (nearly) proportional to UV. As a result, UV generally has smaller effects on exposure ratios between OH and the non-OH reactants. However, under a UV near the lower bound of the explored range in this study ( $< 1 \times 10^{12} \text{ photons cm}^{-2} \text{ s}^{-1}$  at 185 nm) in OFR185, OH production is so small that the effect of  $\text{OHR}_{\text{ext}}$  on OH suppression can be amplified and hence some exposure ratios may be affected. In OFR254 OH is more resilient to suppression even at low UV because of the OH-recycling by initially injected  $\text{O}_3$  (Peng et al., 2015). Note that we call these conditions “riskier” and “safer” mainly in terms of non-tropospheric VOC fate, but not of VOC fate by all non-OH reactants, as some of the non-OH reactant studied in this work may also play a role under some tropospheric conditions (see Sections 3.1.4 and 3.1.5). In addition to the common features above, individual non-OH reactants have their own features as well as**

**a few exceptions to the above mentioned general observations, which we will detail below.”**

We have also made minor modifications throughout the manuscript in accordance with this definition change.

R1.8) 23564/21: “Generation” is a confusing word here, since it usually refers to the number of reactions in a chemical mechanism required to form a specific compound. The more standard term for describing the time to an e-fold of decay is “characteristic lifetime” (e.g., Smith et al., ACP 9, 3209–3222, 2009).

We replace “generation” by “e-fold decay” throughout the ACPD manuscript whenever needed.

R1.9) 23557/section 3.1.5: It should also be noted that ozonolysis can play a major role in the oxidation of dihydrofurans, which can be formed from any number of saturated species, including anthropogenic species. This is described in multiple papers by Ziemann and coworkers; as noted in those papers, OH-only chemistry is not fully representative of the atmospheric conditions in that case, since ozonolysis (or reaction with NO<sub>3</sub>) will dominate the fate of those compounds. This could have substantial implications for SOA formation within the OFR.

We agree with the comment about dihydrofurans that their ozonolysis can play a major role, and thus add a curve, a marker, and data for 4,5-dihydro-2-methylfuran (representative species of dihydrofurans) to Fig. 5, Fig. S5, and Table S3, respectively. We also add the following text to P23558/L23:

**“However, unsaturated oxidation intermediates may have larger contributions from O<sub>3</sub> because of C=C bonds. In particular, dihydrofurans, possible intermediates of saturated hydrocarbon oxidation (Ziemann and Atkinson, 2012; Aimanant and Ziemann, 2013), may be predominantly oxidized by O<sub>3</sub> in the troposphere. In OFR254, they can still have significant contributions from O<sub>3</sub> even outside the low-H<sub>2</sub>O and/or high-OHR<sub>ext</sub> conditions.”**

R1.10) 23558/28 (and elsewhere): Focusing on OH-only chemistry under conditions where OH is not the relevant atmospheric oxidant (such as in the dihydrofuran example above) does not seem to be a very important area of research. It’s unclear to me then why so much text is devoted to discussing how to carry out such experiments.

We underline that it is not possible to replicate the atmosphere in any reactor/chamber. Different experimenters may be interested in different regimes of reactions, and thus will try to isolate those regimes in reactors/chambers by various methods, even though those experiments will not reflect the real atmosphere in a perfectly comprehensive manner. For instance, in chambers OH scavengers are often used to study O<sub>3</sub> reactions to simplify the chemistry under study, or excess NO is added to suppress O<sub>3</sub> and NO<sub>3</sub>, to isolate OH chemistry. In P23558–23559, we

present some guidelines to control the relative importance of OH vs. O<sub>3</sub> oxidation in the reactor. These guidelines will serve to guide experimenters to design experiments that fulfill *their own* objectives.

Therefore, we think that this text is meaningful and keep it. However, for clarity, we have modified the text in P23558/L26 to read:

**“An experimentalist may be interested in obtaining an O<sub>3exp</sub>/OH<sub>exp</sub> in an OFR close to ambient values, which requires lower H<sub>2</sub>O and higher OHR<sub>ext</sub> conditions, although care should be taken to avoid other non-tropospheric reactions under those conditions. On the other hand, one may want to study OH-dominated chemistry and thus want to avoid significant ozonolysis of VOCs to reduce the complexity of VOC fate. This is analogous to the addition of excess NO to suppress O<sub>3</sub> in some chamber experiments.”**

R1.11) 23560/8: This paragraph neglects what may be the most interesting/important aspect of HO<sub>2</sub> chemistry, the formation of HO<sub>2</sub>-carbonyl adducts (to form hydroxyhydroperoxy radicals). Under the very high HO<sub>2</sub> concentrations of the OFR, these may then form hydroxyhydroperoxides, probably to a higher extent than would happen in the troposphere. This channel should be explored here.

In this paper, we focus on the fate of stable species in OFRs only, as there are many other issues that concern the fate of peroxy radicals in OFRs, as also discussed in response to comment R1.4. We plan to explore those issues in a separate publication. Nevertheless, carbonyl compounds can be stable species. We thus briefly discuss their fate by reaction with HO<sub>2</sub> and modify the text to P23560/L9 to read:

**“Typically, the rate constants of reactions of HO<sub>2</sub> with alkenes are smaller than 10<sup>-20</sup> cm<sup>3</sup> molecule<sup>-1</sup> s<sup>-1</sup> at room temperature, and those with almost all saturated VOCs (except aldehydes and ketones) are even smaller (Tsang, 1991; Baulch et al., 1992, 2005). Therefore, we briefly discuss reactions of HO<sub>2</sub> with aldehydes and ketones, and neglect those with all other VOCs in this study. Ketones react with HO<sub>2</sub> at rate constants on the order of 10<sup>-16</sup> cm<sup>3</sup> molecule<sup>-1</sup> s<sup>-1</sup> or lower (Gierczak and Ravishankara, 2000; Cours et al., 2007). Therefore, only at low H<sub>2</sub>O, low UV and high OHR<sub>ext</sub>, the reaction of acetone with HO<sub>2</sub> may compete with that with OH. The same is likely true for the reactions of acetaldehyde and larger aldehydes with HO<sub>2</sub>, as their rate constants are likely to be around or less than 1x10<sup>-14</sup> cm<sup>3</sup> molecule<sup>-1</sup> s<sup>-1</sup> (da Silva and Bozzelli, 2009). Formaldehyde is the only stable carbonyl compound that may react with HO<sub>2</sub> (rate constant: 7.9x10<sup>-14</sup> cm<sup>3</sup> molecule<sup>-1</sup> s<sup>-1</sup>; Ammann et al., 2015) at a rate competing with that with OH under conditions that are not low-H<sub>2</sub>O, low-UV, and high-OHR<sub>ext</sub>. Note that the reaction of formaldehyde with HO<sub>2</sub> is also significant in the atmosphere (Pitts and Finlayson, 1975; Gäb et al., 1985). However, its product, hydroxymethylperoxy radical, dominantly undergoes decomposition via thermal reaction and photolysis (Kumar and Francisco, 2015), compared to the hydroxymethylhydroperoxide formation pathway via a further reaction with HO<sub>2</sub> (Ziemann and Atkinson, 2012). Even if hydroxymethylhydroperoxide is**

**produced in appreciable amounts, in the high-OH environment of OFRs, this species can be easily predicted to convert into formic acid (Francisco and Eisefeld, 2009) and eventually CO<sub>2</sub>. All these products have very few interactions with other VOCs, and hence should not significantly perturb the reaction system of OFRs.”**

R1.12) Table S6: Presumably these are intended to be “surrogate” SOA components, not “possible” ones, since most are far too volatile to be in the condensed phase.

This is indeed the case. We have replaced “possible” in P23563/L11 and the caption of Table S6 in the ACPD paper by “surrogate”.

## Anonymous Referee #2

Peng et al. conduct a modeling study to examine the importance of UV photolysis as well as  $O_3$ ,  $O(^1D)$ , and  $O(^3P)$  reactions relative to OH reactions in oxidation flow reactors (OFRs). Overall, this manuscript addresses important issues regarding the application of oxidation flow reactors to examine OH oxidation chemistry in targeted laboratory and field studies. The authors examine a wide range of operating conditions in flow reactors and identify a subset of “optimal” and “pathological” conditions. Before the manuscript can be considered for publication in ACP, significant rewriting/reorganization is required to more clearly present and discuss the implications of the modeling work. Specific comments and suggestions are listed below.

R2.1) F185, F254,  $O(^1D)$  exposure, and  $O(^3P)$  exposure are all correlated with OH exposure to some extent, yet the modeling work in this manuscript suggests it is possible to vary  $F185/OH_{exp}$ ,  $F254/OH_{exp}$ ,  $O(^1D)_{exp}/OH_{exp}$ , and  $O(^3P)_{exp}/OH_{exp}$  over orders of magnitude range by varying the water vapor mixing ratio, photon flux, and external OH reactivity. To provide useful context/introduction to Figures 1-5, I suggest parameterizing these ratios as a function of input OFR conditions, because in its current form the manuscript mostly uses qualitative statements relating high  $F185/OH_{exp}$ ,  $F254/OH_{exp}$ ,  $O(^1D)_{exp}/OH_{exp}$ , and  $O(^3P)_{exp}/OH_{exp}$  values to “pathological conditions”.

For example, plotting (i)  $F185/OH_{exp}$  (ii)  $F254/OH_{exp}$  (iii)  $O(^1D)_{exp}/OH_{exp}$  (iv)  $O(^3P)_{exp}/OH_{exp}$  versus  $OHR_{ext}/[H_2O]$  – or a similar combination of input parameters that incorporate correlation of  $F185/OH_{exp}$  with  $OHR_{ext}$  and anti-correlation with  $H_2O$  – over appropriate range of  $OHR_{ext}$  and  $[H_2O]$ . Individual traces could be shown corresponding to “L”, “M”, “H” photon fluxes displayed in Table 1 for “OFR185”, “OFR254-7” and “OFR254-70” as appropriate. These figures could allow for quantitative comparison of, for example:  $[H_2O] = 2.3\%$  at  $OHR_{ext} = 1000\text{ s}^{-1}$  versus  $[H_2O] = 0.07\%$  at  $OHR_{ext} = 0\text{ s}^{-1}$ , as well as other intermediate conditions that are for the most part not considered in the manuscript. Presumably these plots can be derived from the model simulation data that has already been obtained, and perhaps consolidated into a single figure with a few subpanels.

We agree that a parameterization of those exposures would be very practical for future studies, and thank the reviewer for the suggestion. Thus we have derived estimation equations for  $O(^1D)_{exp}$ ,  $O(^3P)_{exp}$ , and  $O_{3exp}$  in both OFR185 and OFR254.  $F185_{exp}$  and  $F254_{exp}$  can be regarded as input experimental conditions. Therefore, all exposure ratios of these species can now be obtained. To document the details of these estimation equations, we have added a section in Supp. Info. to read:

### “S3. Estimation equations of non-OH reactant exposures

In order that one may practically estimate exposure ratios between non-OH reactants and OH under any condition for OFR operation, we provide the estimation equations of  $O(^3P)$ ,  $O(^1D)$ , and  $O_3$  exposures obtained by fitting the modeling results (Table S9). The equations for OFR254 are fitted from the results of the same runs as in Peng et al. (2015b), while those for OFR185 from the modeling data under conditions spanning the

same H<sub>2</sub>O, UV, and OHR<sub>ext</sub> ranges as for OFR254, but without the initial O<sub>3</sub> (O<sub>3,in</sub>) dimension. Exposures estimated from these equations compare very well with the modeled exposures (Fig. S6). Scatter plots between a few exposures are also shown in Fig. S6.

For OFR254, UV at 254 nm can be estimated by collectively considering and solving Eqs. 11 and 12 in Peng et al. (2015b), if rO<sub>3</sub> (i.e., ratio between O<sub>3</sub> at the reactor entrance and exit) is known, and vice versa. For OFR185, one of UV at 185 nm and O<sub>3exp</sub> (or average O<sub>3</sub>) can be obtained if the other is known according to Eq. S1 below. UV at 254 nm in OFR185 can be calculated by Eq. S1 in Li et al. (2015), and then photon flux exposures can be easily estimated.

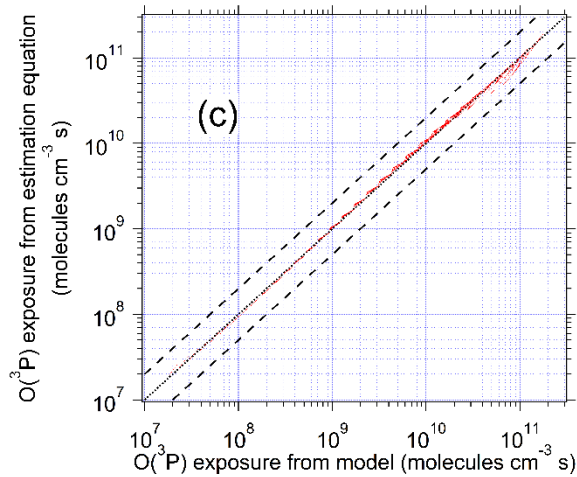
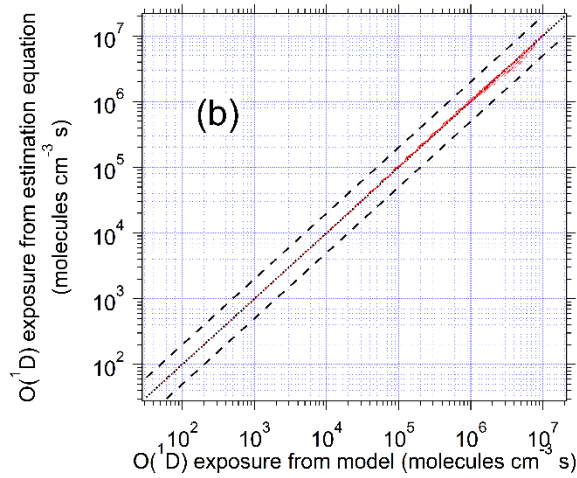
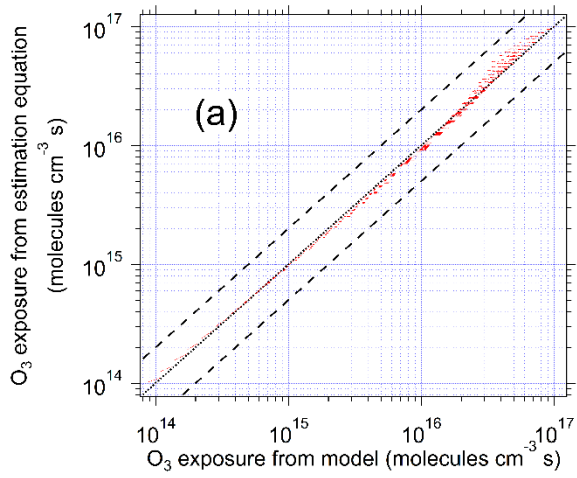
The ratios of F185 and F254 exposures to OH exposure are the most important parameter in this work that determine the relative contribution of non-tropospheric VOC photolysis. Therefore, we also provide equations for directly estimating these parameters from measurable surrogates of UV (i.e., O<sub>3exp</sub> in OFR185 and rO<sub>3</sub> in OFR254) (Table S9 and Fig. S6).

Table S9. Estimation equations of O(<sup>3</sup>P), O(<sup>1</sup>D), and O<sub>3</sub> exposures and ratios of F254<sub>exp</sub> to OH<sub>exp</sub> for both OFR185 and OFR254, and ratio of F185<sub>exp</sub> to OH<sub>exp</sub> for OFR185. UV in the equations for OFR185 and OFR254 are the photon fluxes at 185 and 254 nm, respectively. Numbers of fitted datapoints and average absolute value of the relative deviations (AAVRD) of the estimates by the equations from the fitted datapoints are also shown. rO<sub>3</sub> is the ratio between O<sub>3</sub> at the reactor exit and entrance. For OFR254, one of rO<sub>3</sub> and UV can be obtained by collectively considering and solving Eqs. 11 and 12 in Peng et al. (2015b) if the other is known. OH, O<sub>3</sub>, O(<sup>1</sup>D), and O(<sup>3</sup>P) exposures are in molecules cm<sup>-3</sup> s, F185<sub>exp</sub> and F254<sub>exp</sub> in photons cm<sup>-2</sup>, OHR<sub>ext</sub> in s<sup>-1</sup>, UV in photons cm<sup>-2</sup> s<sup>-1</sup>, O<sub>3,in</sub> in ppb, and H<sub>2</sub>O and rO<sub>3</sub> unitless.

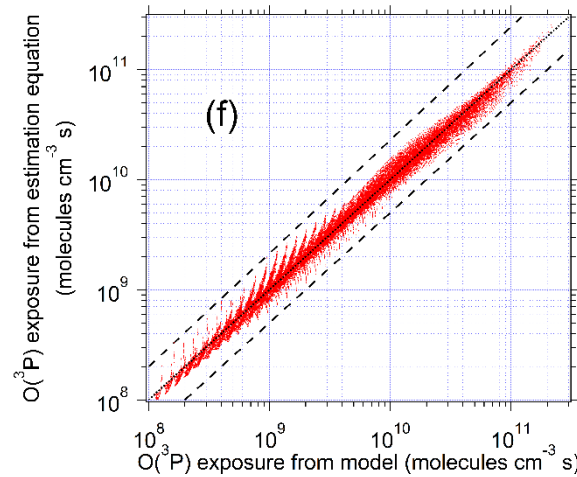
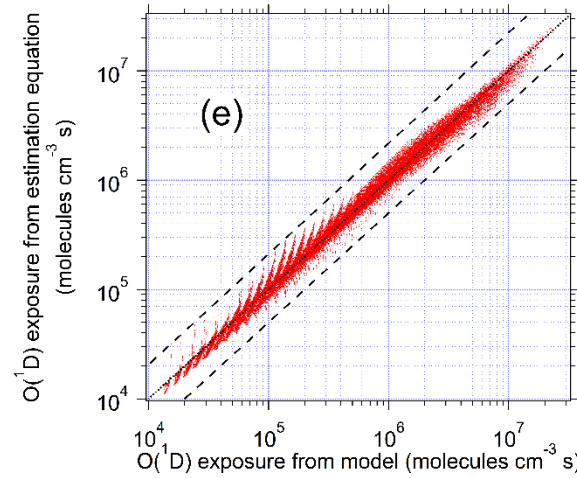
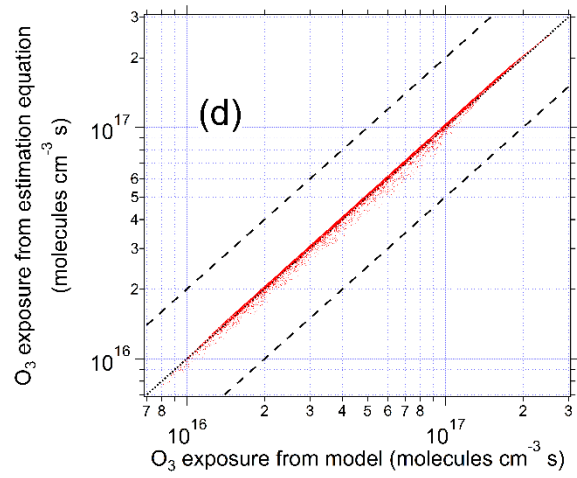
OFR type	Eq. No.	Estimation equation	Number of fitted data-points	AAVRD (%)
OFR185	S1	$\log O_{3exp} = 3.1825 + 0.98741 \log UV + 40.352H_2O - 3.8184H_2O \cdot \log UV$	28800	6
	S2	$\log O(^3P)_{exp} = 313.61 - 558.66 \log(\log O_{3exp}) - 171.59H_2O + 254.33(\log(\log O_{3exp}))^2 + 147.27H_2O \cdot \log(\log O_{3exp})$		6
	S3	$\log O(^1D)_{exp} = 90.595 - 208.28 \log(\log O_{3exp}) - 155.9H_2O + 114.15(\log(\log O_{3exp}))^2 + 134.4H_2O \cdot \log(\log O_{3exp})$		4

	<b>S4</b>	$\log(F185_{\text{exp}}/OH_{\text{exp}})$ $= -2.7477 - 0.79645 \log H_2O + 0.25018 \log O_{3\text{exp}}$ $+ 3.8051 \log OHR_{\text{ext}} - 0.22685 \log OHR_{\text{ext}} \cdot \log O_{3\text{exp}}$ $+ 0.0086381(\log OHR_{\text{ext}})^2 \cdot \log O_{3\text{exp}}$		<b>14</b>
	<b>S5</b>	$\log(F254_{\text{exp}}/OH_{\text{exp}})$ $= 3.325 - 0.8268 \log H_2O$ $+ 3.7467 \log OHR_{\text{ext}} - 0.22294 \log OHR_{\text{ext}} \cdot \log O_{3\text{exp}}$ $+ 0.0086345(\log OHR_{\text{ext}})^2 \cdot \log O_{3\text{exp}}$		<b>14</b>
<b>OFR254</b>	<b>S6</b>	$\log O_{3\text{exp}} = 15.559 + \log O_{3,\text{in}} + 0.42073 \log rO_3$	<b>316800</b>	<b>1</b>
	<b>S7</b>	$\log O(^3P)_{\text{exp}} = 7.6621 + 0.16135 \log(-\log rO_3)$ $- 1.1342 \log H_2O + 0.59182 \log O_{3,\text{in}}$ $- 0.17007 \log H_2O \cdot \log(-\log rO_3)$ $- 0.3797(\log(-\log rO_3))^2$ $+ 0.099902 \log OHR_{\text{ext}}$		<b>5</b>
	<b>S8</b>	$\log O(^1D)_{\text{exp}} = 3.7371 + 0.1608 \log(-\log rO_3)$ $- 1.1344 \log H_2O + 0.59179 \log O_{3,\text{in}}$ $- 0.17019 \log H_2O \cdot \log(-\log rO_3)$ $- 0.37983(\log(-\log rO_3))^2$ $+ 0.099941 \log OHR_{\text{ext}}$		<b>5</b>
	<b>S9</b>	$\log(F254_{\text{exp}}/OH_{\text{exp}})$ $= 2.8045 - 0.888519 \log H_2O$ $- 0.015648 \log(-\log rO_3)$ $- 0.2607 \log OHR_{\text{ext}} - 0.1641(\log(-\log rO_3))^2$ $+ (OHR_{\text{ext}}/O_{3,\text{in}})^{0.25142}$		<b>14</b>

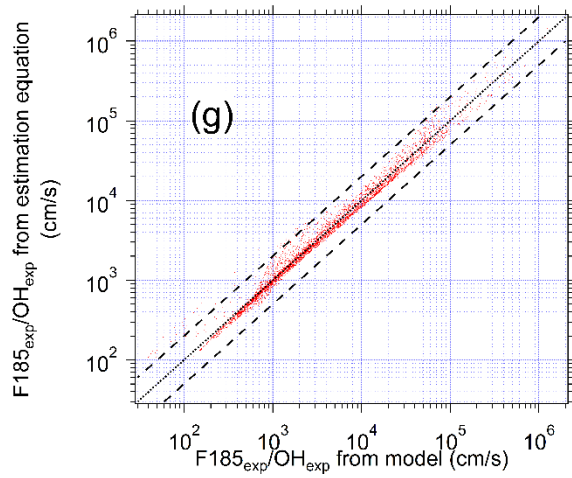
# OFR185



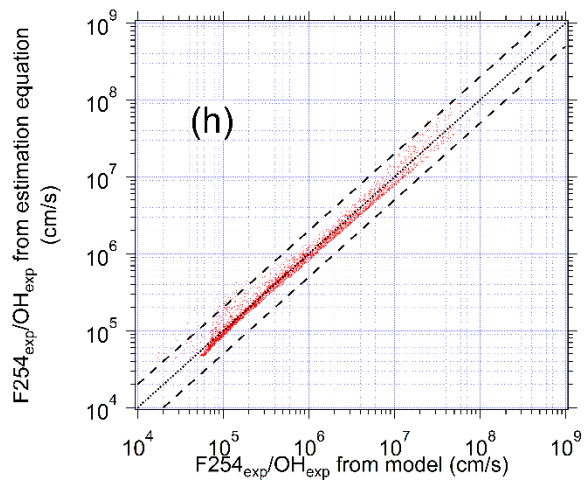
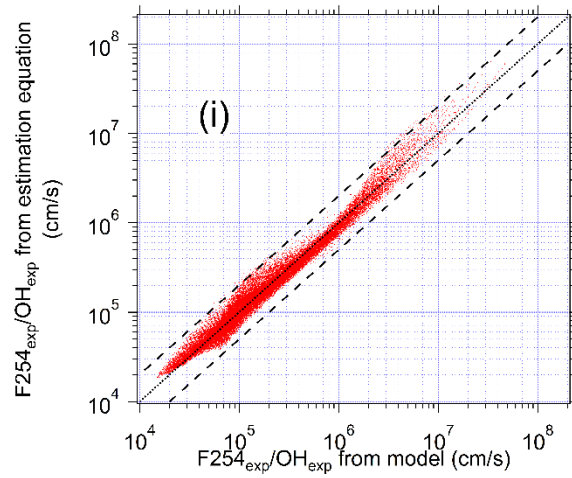
# OFR254



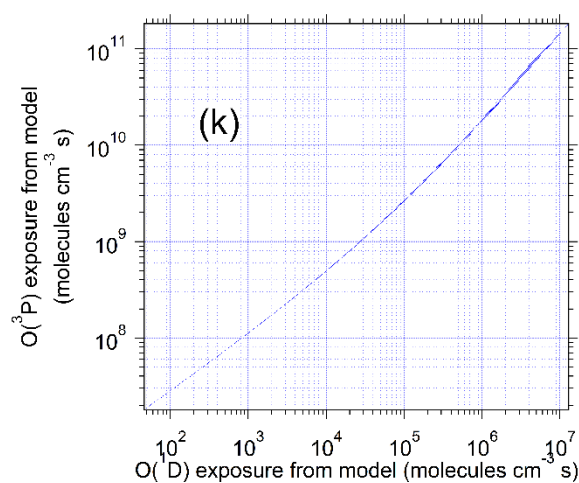
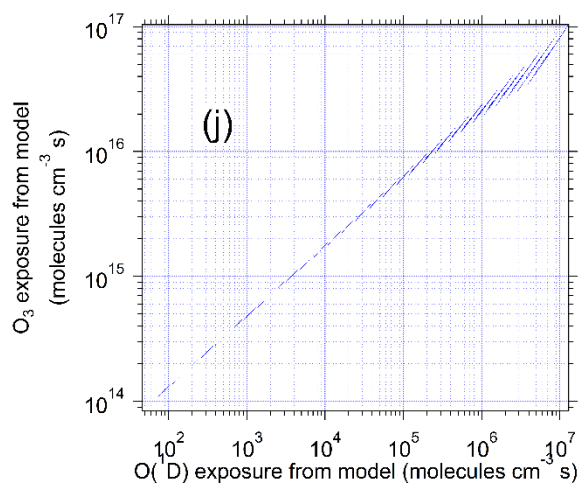
# OFR185



# OFR254



## OFR185



## OFR254

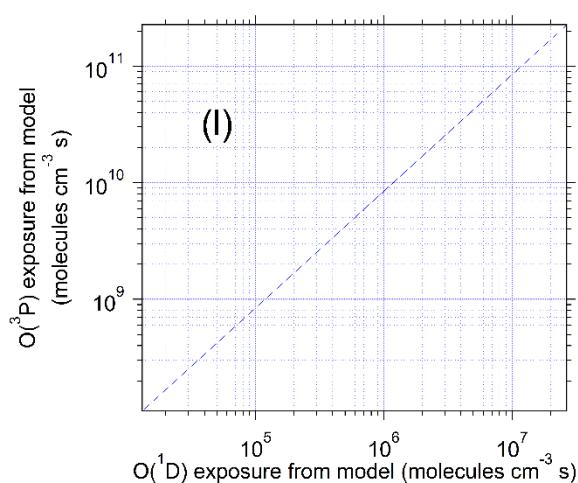


**Figure S6. O<sub>3</sub>, O(<sup>1</sup>D), and O(<sup>3</sup>P) exposures and ratios of F185 and F254 exposures to OH exposure from estimation equations vs. those from the model for (a–c, g, h) OFR185 and (d–f, i) OFR254. 1:1 (dotted), 1:2, and 2:1 (dashed) lines are shown in (a–i) to facilitate comparison. Scatter plots between modeled exposures for (j, k) OFR185 and (l) OFR254 are also shown.**

We have also added the following paragraph to P23556/L21 to read:

“OFR experiments can be simply conducted under safer conditions to avoid non-tropospheric VOC fate, while riskier conditions can lead to significant non-tropospheric VOC fate, depending on the species under study. The conditions in between, i.e., “transition” conditions, are explicitly discussed above. However, one may want to be able to more quantitatively estimate the relative importance of non-OH reactants under different conditions so that a more detailed experimental planning becomes possible that simultaneously ensures insignificant non-tropospheric VOC fate and specific experimental goals. For this purpose, we provide a series of estimation equations for

**non-OH reactant exposures (Section S3, Table S9, and Fig. S6, as well as Excel file). With these equations, the relative contribution of non-OH reactants under all conditions explored in this study can be easily estimated. In OFR studies where a different OFR design is adopted and/or chemistry beyond the approximations in our model is involved, a new model may need to be established, which can be done in similar manner as Peng et al. (2015), to obtain the relative importance of non-OH VOC fate and then perform experimental design.”**

Regarding the consolidation of figures, see responses to R1.7 and R2.2.

R2.2) Figures 1-5 are too difficult to read and interpret. There is too much data shown here – 28 compounds in Figure 1, 29 compounds in Figure 2, 9 compounds in Figure 3, 32 compounds in Figure 4, and 25 compounds in Figure 5 – making the figures overwhelming to the point of not being useful, especially with the histograms and insets that are also displayed in the figures.

See response to R1.7. Also note that all curves for all the compounds all have the same shape and only differ in their X-axis offset. To further facilitate reading, all species in the legend are sorted by the fractional importance of their non-OH fate, and several species categories of particular interest (e.g., aromatics and ketones in Fig. 2) are denoted with markers. Thus, although that Figs. 1–5 are complex, we think that this level of complexity is needed to serve as a useful reference for future studies.

R2.3) The “fractional importance of X” (X = F185, F254, O(<sup>1</sup>D), O(<sup>3</sup>P), O<sub>3</sub>) curves are derived from the literature rate constants and absorption cross sections that are summarized in Tables S1 and S2. Since they only serve as qualitative reference points to interpret the modeling results, it would be sufficient to show them only in Figures S1-S5 and reference as needed in the text, which could be cut back a bit. This might also make Figures 1-5 compact enough to consolidate into two figures, perhaps one with two subpanels (F185/OH<sub>exp</sub> and F254/OH<sub>exp</sub>), and the other with three subpanels (O(<sup>1</sup>D)<sub>exp</sub>/OH<sub>exp</sub>, O(<sup>3</sup>P)<sub>exp</sub>/OH<sub>exp</sub>, O<sub>3exp</sub>/OH<sub>exp</sub>).

See responses to R1.7 and R2.2. Figures 1–5 were designed as they are in order that readers can straightforwardly evaluate various non-OH destruction pathways of specific (categories of) compounds under different conditions in OFRs, and easily relate them to field, source, and laboratory studies, which are key goals of this paper. We believe that curves and insets in Figs. 1–5 carry necessary information and cannot be substantially reduced or simplified without major loss of information.

R2.4) It is not clear how to quantitatively interpret the CalNex, SOAS and BEACHON histograms because they are shrunk to a minimal size to make room for the X/(X + OH) curves. If they have a labeled ordinate, it is not clear to me what it is. Also, even though it is stated in the figure captions that “all curves, markers, and histograms share the same abscissa” (not the same ordinate) the natural tendency is to look at Figure 1, for example, and assume that  $j_{185}/(j_{185} + k_{OH}[OH]) > 20\%$  for the field studies and  $j_{185}/(j_{185} + k_{OH}[OH]) \sim 75\%$  for the source studies.

We apologize for omitting the Y-axis for these histograms, and we realize how this could be confusing. The relevant ordinate for these histograms is the fractional occurrence of a given condition ( $X_{\text{exp}}/OH_{\text{exp}}$ ) in each field study. We have added these axes in the revised version of the figures.

We have also added explanations and modified the text in the relevant figure captions for clarity, e.g., in the caption of Fig. 1:

**“The lower inset shows histograms of model-estimated F185/OH exposures for three field studies where OFR185 was used to process ambient air. Their ordinate is the fractional occurrence of a given condition ( $X_{\text{exp}}/OH_{\text{exp}}$ ). All histograms are normalized to be of identical total area (i.e., total probability of 1). The upper inset (black and blue markers) shows similar information for source studies of biomass smoke (FLAME-3; Ortega et al., 2013) and an urban tunnel (Tkacik et al., 2014). All curves, markers, and histograms in this figure share the same abscissa.”**

R2.5) I would like to see more discussion of the characteristic features of the histograms displayed in Figures 1-5 and what causes them differ from one campaign to the next. For example, in Figure 1, there appears to be two distinct clusters of F185/ $OH_{\text{exp}}$  in the SOAS campaign, whereas there is a wider band of F185/ $OH_{\text{exp}}$  in CalNex. Then, in Figure 2, the SOAS dataset has a wider range of F254/ $OH_{\text{exp}}$  than the CalNex dataset. What specific ambient or OFR conditions yield these results?

These histograms are model outputs, which have a complex dependence on ambient temperature,  $OHR_{\text{ext}}$ , and  $H_2O$ , as well as on the UV lamp settings used for each campaign etc. Differences in these histograms for different campaigns, is both due to ambient variations (temperature,  $OHR_{\text{ext}}$ , and  $H_2O$ ) and experimental setup (UV settings). We have added a mention of this to P23550/L20:

**“Note that the outputs for field studies, i.e., histograms, have a complex dependence on ambient temperature,  $H_2O$ , and  $OHR_{\text{ext}}$ , as well as UV steps used. The specific histogram shapes for different field campaigns are influenced by both ambient and experimental parameters.”**

Exploring this issue in the revised paper would require quite a bit more space and would appear to be of very narrow interest. We thus refrain from doing so in the revised manuscript. We can provide further details upon request.

R2.6) The results shown in Figure 6 would be more useful if displayed in a table format with columns: Species, Ambient photolysis %, OFR185 photolysis %, OFR254-70 photolysis %. Figure 6 is too busy/cluttered with all of the tags, and it is impossible to decipher the OFR photolysis percentages below the 1:100 and 1:1000 lines.

We have added the requested table to Supp. Info. (Table S5). However we prefer to keep the information in graphical form in the main paper, which is much superior for communication purposes to a table format, in our experience. We have relocated some of the tags to reduce clutter and make the figure easier to read. The new table and figure are reproduced below.

Table S5. Absorption cross-sections at 185 and 254 nm for several atmospheric oxidation intermediates from Keller-Rudek et al. (2015), ambient photolysis rate constants from Hodzic et al. (2015), and photolysis percentages in OFR185 and OFR254-70 (under the condition of 70% relative humidity and 25 s<sup>-1</sup> initial OHR<sub>ext</sub>) and in the troposphere at an OH exposure equivalent to a photochemical age of 1 week (assuming an ambient OH concentration of 1.5x10<sup>6</sup> molecules cm<sup>-3</sup>). “N/A” in the table stands for “not available”.

Species	Cross-sections (cm <sup>2</sup> )		Ambient photolysis rate constant (s <sup>-1</sup> )	Photolysis percentage		
	185 nm	254 nm		OFR185	OFR254-70	Ambient
acrolein	2.82E-17	7.00E-22	1.39E-06	4.1	0.002	57
methacrolein	6.77E-18	1.78E-21	1.34E-05	1.0	0.005	100
acetone	2.91E-18	3.01E-20	3.82E-07	1.1	0.083	21
biacetyl	1.46E-18	3.71E-20	2.29E-04	1.0	0.103	100
pyruvic acid	N/A	1.61E-20	1.03E-04	N/A	0.045	100
methyl vinyl ketone	N/A	2.41E-21	4.72E-06	N/A	0.007	94
methylglyoxal	N/A	2.76E-20	7.79E-05	N/A	0.076	100
hydroxyacetone	5.40E-18	5.07E-20	1.51E-06	1.9	0.140	60
2,4-dimethyl-3-pentanone	N/A	1.66E-20	8.30E-06	N/A	0.046	99
2-methylpropanal	5.71E-18	1.22E-20	3.80E-05	1.1	0.034	100
4-methyl-2-pentanone	N/A	2.75E-20	5.48E-06	N/A	0.076	96
5-methyl-2-hexanone	N/A	2.39E-20	4.34E-06	N/A	0.066	93
2-propyl nitrate	1.79E-17	4.86E-20	1.93E-06	3.7	0.135	69
crotonaldehyde	1.05E-17	2.80E-21	9.87E-06	1.6	0.008	100
acetaldehyde	7.83E-20	1.57E-20	3.51E-06	0.4	0.044	88
3-pentanone	N/A	3.00E-20	3.07E-06	N/A	0.083	84
methyl ethyl ketone	1.31E-18	3.09E-20	2.98E-06	0.9	0.086	83
propanal	1.42E-17	1.75E-20	1.30E-05	2.5	0.048	100
n-butanal	7.99E-18	1.45E-20	1.14E-05	1.5	0.040	100
n-pentanal	N/A	1.43E-20	1.63E-06	N/A	0.040	63
n-hexanal	N/A	1.14E-20	1.18E-05	N/A	0.032	100
1-butyl nitrate	1.81E-17	4.60E-20	1.71E-06	3.6	0.127	64
1-propyl nitrate	1.81E-17	4.40E-20	1.84E-06	3.6	0.122	67
ethyl nitrate	1.71E-17	4.10E-20	1.16E-06	3.4	0.114	50
methyl nitrate	2.10E-17	3.34E-20	7.27E-07	3.8	0.093	36
methylhydroperoxide	9.00E-19	3.23E-20	4.25E-06	0.9	0.089	92
glyoxal	4.80E-19	1.59E-20	4.72E-04	0.4	0.044	100
peroxyacetyl nitrate	6.20E-18	1.00E-19	6.24E-07	3.1	0.277	31
glycolaldehyde	3.85E-18	3.76E-20	6.82E-06	1.4	0.104	98
hydroxymethyl hydroperoxide	N/A	2.88E-20	3.90E-06	N/A	0.080	91

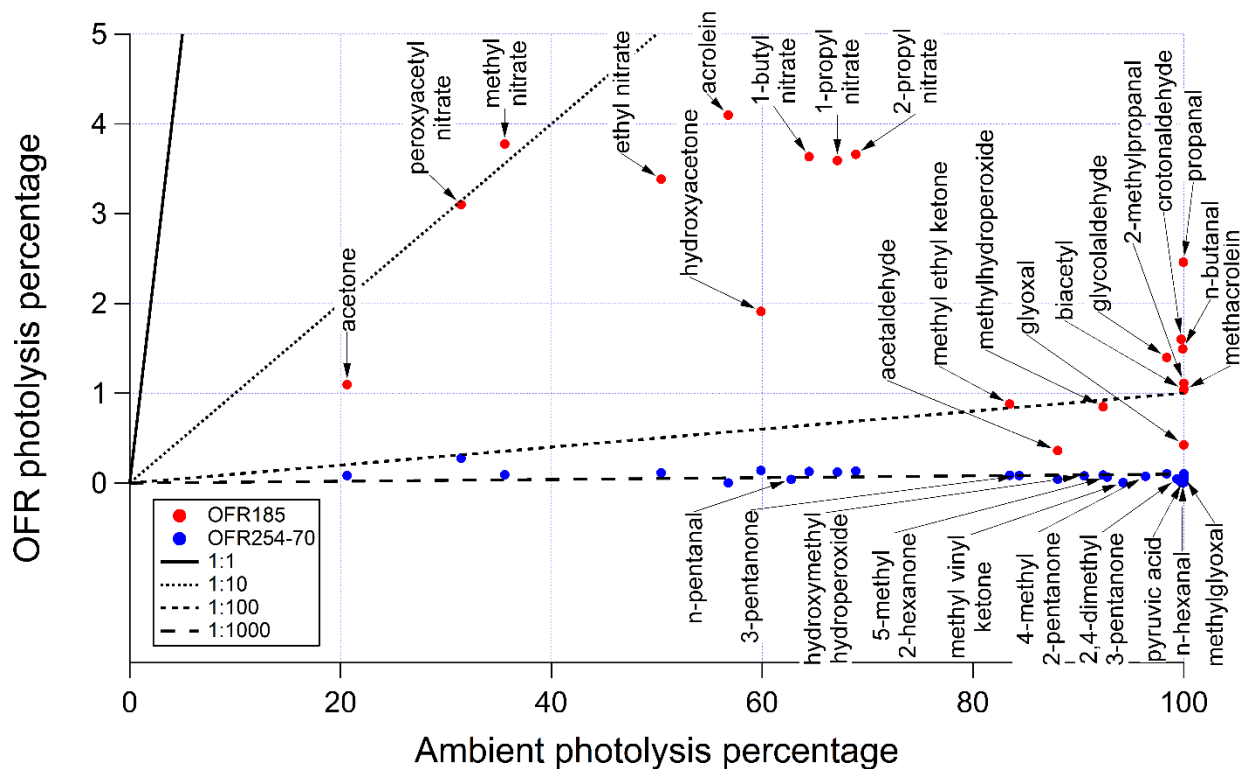


**Figure 6. Ambient photolysis fractions of secondary species in a week (calculated from photolysis rates reported in Hodzic et al. (2015)) vs. photolysis fractions of those species in OFR185 and OFR254-70 when reaching the same photochemical age (ambient OH concentration of  $1.5 \times 10^6$  molecules  $\text{cm}^{-3}$  assumed) under conditions of 70% relative humidity (water vapor mixing ratio of 1.4%) and  $25 \text{ s}^{-1}$  initial  $\text{OHR}_{\text{ext}}$ . If the points of a certain species for both OFR185 and OFR254-70 are available, the species name is tagged on the OFR185 point (downward arrow), otherwise on the OFR254-70 point (upward arrow). The 1:1, 1:10, 1:100, and 1:1000 lines are also shown for comparison.**

R2.7) P23653 and Figure 8: “We use surrogate gas-phase species for the different functional groups as the cross sections of SOA-relevant species at these wavelengths are not available.” There are at least two literature studies reporting SOA absorption cross-sections down to  $\lambda = 300 \text{ nm}$  (Updyke et al., 2012; Lambe et al. 2013; both of which report absorption Angstrom exponents that can be used to extrapolate down to  $\lambda = 254 \text{ nm}$ ), at least one study reporting SOA absorption cross sections down to  $\lambda = 250 \text{ nm}$  (Romonosky et al., 2015), and at least two literature studies that report SOA absorption cross sections down to  $\lambda = 220 \text{ nm}$  (Liu et al., 2013; Liu et al., 2015):

- Updyke et al., 2012: SOA generated from OH oxidation of naphthalene and cedar leaf oil
- Lambe et al., 2013: SOA generated from OH oxidation of  $\alpha$ -pinene, tricyclo[5.2.1.0<sup>2,6</sup>]decane, naphthalene, and guaiacol
- Romonosky et al., 2015: SOA generated from ozonolysis and OH oxidation of isoprene and  $\alpha$ -pinene, and OH oxidation of m-xylene. There are 25 total SOA systems with reported absorption cross sections down to approx.  $\lambda = 280 \text{ nm}$ ).

- Liu et al., 2013: SOA generated from ozonolysis of  $\alpha$ -pinene, limonene and catechol
- Liu et al., 2015: SOA generated from OH oxidation of toluene and m-xylene

All of these studies should be referenced in the Section 3.2 text, and a representative subset of the data should be incorporated into Figure 8.

[See a detailed response to this issue in response to comment R1.1.3.](#)

R2.8) Figure 8 and related discussion: aside from sulfuric acid, glyoxal, and nitric acid, virtually all of the individual compounds shown in this plot are either already presented on similar axes in Fig. 1, 2, S1 and S2, and/or are too volatile to participate in SOA formation processes. Thus, they are not relevant surrogate compounds for SOA. While it is true that  $\lambda = 185$  nm absorption cross sections are available for these compounds but not for SOA, the authors have already shown that the trends at  $\lambda = 185$  nm and  $\lambda = 254$  nm relative to  $\text{OH}_{\text{exp}}$  are similar. In this figure and related discussion, I suggest only showing relative photolysis rates at 254 nm for the SOA systems outlined in Comment #7, then if needed briefly mention in the text that the 185 nm results are expected to be similar.

[See response to comment R1.1.3.](#)

R2.9) Section 3.2: To supplement Figure 7, where the effects of (1) increasing RH from 3% to 60% in a laboratory SOA experiment and (2) diluting sample in two source measurements are shown, I would like to see an example of how humidifying an ambient sample to  $[\text{H}_2\text{O}] = 2.3\%$  prior to introduction to the OFR influences the  $F_{185}/\text{OH}_{\text{exp}}$  and/or  $F_{254}/\text{OH}_{\text{exp}}$  histograms of one of the field studies shown in Figures 1-5. While the field measurements are generally not subject to “pathological conditions” as defined by the authors, this analysis would quantitatively demonstrate the efficacy of minimizing non-OH chemistry in OFRs using one of the suggested improvements in experiment design.

[We can add an example in the paper to show the effect of humidifying an ambient sample to  \$\text{H}\_2\text{O} = 2.3\%\$  on  \$X\_{\text{exp}}/\text{OH}\_{\text{exp}}\$ . However, this cannot be done as suggested by the Referee, since the saturated water vapor mixing ratio during the night was often lower than 2.3% in these field campaigns, while ambient  \$\text{H}\_2\text{O}\$  during the day was sometimes higher than 2.3%. Even if the humidification is always done to near water vapor saturation, its effect still depends on relative humidity prior to humidification, temperature, and pressure, which differ for all datapoints of ambient measurements. As a result, this effect can only be quantitatively assessed under specific conditions. Therefore, we take the average condition of the BEACHON-RoMBAS study as the reference, whose temperature, pressure,  \$\text{OHR}\_{\text{ext}}\$ , relative humidity etc. are fixed \(Table S4\). Then the quantitative comparison of the reference condition with the humidified condition \( \$\text{H}\_2\text{O} = 2.3\%\$ \) becomes possible.](#)

[We add the data corresponding to the humidified condition to Table S4 and the text in P23565/L21 to read:](#)

**“Humidifying the average condition of the BEACHON-RoMBAS (Palm et al., 2016) campaign from H<sub>2</sub>O = 1.6% (RH = 63%) to H<sub>2</sub>O = 2.3% (RH = 92%) leads to significant (from ~20% for 185 nm photon flux to a factor of ~3 for O(<sup>3</sup>P)) decreases in all exposure ratios between non-OH reactants and OH (Table S4).”**

R2.10) Water vapor concentrations are discussed in terms of both mixing ratio and relative humidity. It would be preferable to choose one or the other and stick with that throughout the manuscript.

We change all “relative humidity” or “RH” to “water vapor mixing ratio” or “H<sub>2</sub>O” in the manuscript, except when specific relative humidity values mentioned in the discussion related to previous OFR studies. In those cases we add the corresponding water vapor mixing ratios in parentheses for clarity, e.g., in P23565/L19 to read:

**“For example, increasing RH from 3% to 60% (H<sub>2</sub>O from ~0.06% to ~1.2%) lowers the percentage of non-tropospheric consumption of p-xylene in Kang et al. (2011)’s mixture experiment from ~20% to 1.5%.”**

R2.11) P23545, L17: Quantify “low RH” and “high OHR<sub>ext</sub>”.

We have given a clearer definition of these conditions above (see response to R1.7), and modify the text in P23545/L16 to read:

**“We define “riskier OFR conditions” as those with either low H<sub>2</sub>O (<0.1%) or high OHR<sub>ext</sub> (≥100 s<sup>-1</sup> in OFR185 and >200 s<sup>-1</sup> in OFR254). We strongly suggest avoiding such conditions as the importance of non-OH reactants can be substantial for the most sensitive species, although depending on the species present OH may still dominate under some riskier conditions.”**

R2.12) P23545, L21: Quantify “low O<sub>2</sub>”.

We modify the text in P23545/L16 to read:

**“Working under low O<sub>2</sub> (volume mixing ratio of 0.002) with the OFR185 mode allows OH to completely dominate over O<sub>3</sub> reactions even for the biogenic species most reactive with O<sub>3</sub>.”**

R2.13) P23545, L26-28: “SOA photolysis is shown to be insignificant for most functional groups, except for nitrates and especially aromatics, which may be photolyzed at high UV flux settings.” Quantify “insignificant”, “high UV flux”, and the extent of photolysis that is deemed significant at the high UV flux.

We have modified this sentence above (see response to R1.1.3). In the revised sentence, “significant”, “high UV flux” etc. have been quantified.

R2.14) P23545-6, L28-2: *“The results allow improved OFR operation and experimental design, as well as guidance for the design of future reactors.”* Briefly summarize the suggested improvements, which include (1) maximizing [H<sub>2</sub>O] (2) minimizing OHR<sub>ext</sub> through sample dilution and (3) operating OFR254 at [O<sub>3</sub>] ~ 70 ppm rather than ~7 ppm. Also, while there is extensive discussion of how to improve OFR operation and experiment design, I did not notice any discussion in the manuscript about “guidance for the design of future reactors” – either delete this text or add specific suggestions for how to improve future reactor design.

We already stated in P23545/L23 that *“Non-tropospheric VOC photolysis may have been a problem in some laboratory and source studies, but can be avoided or lessened in future studies by diluting source emissions and working at lower precursor concentrations in lab studies, and by humidification.”* Significant non-tropospheric VOC photolysis should be avoided, which can be done by increasing H<sub>2</sub>O and/or lowering OHR<sub>ext</sub>. It is not always desirable to avoid all non-OH VOC fates, as some actually also occur in the atmosphere, and rather this aspect should be part of the experimental design (see responses to R1.3, R1.9, and R1.10). Although increasing H<sub>2</sub>O and/or lowering OHR<sub>ext</sub> may achieve frequent goals/conditions, we did not and should not recommend specific approaches for *all purposes*.

For clarity, we modify the sentence quoted by the Referee in P23545/28 to read:

**“The results of this study allow improved OFR operation and experimental design, and also inform the design of future reactors.”**

R2.15) P23548, L5: “...whose intensity can be rapidly computer-controlled.” This seems like extraneous detail to include - consider deleting.

The fact that UV lamp setting can be rapidly computer-controlled is not an extraneous detail but an important and relevant one. It highlights the convenience of conducting UV-controlled OFR experiments and the possibility of rapidly scanning UV lamp settings during an experiment. In particular, the latter has unique applications to OFR experiments in field studies. In these experiments, OFRs enable the exploration of a very large range of photochemical age during a short period when ambient conditions usually do not significantly change. Therefore, we keep this sentence as it is.

To clarify this point, we add the following text to P23549/L17:

**“Rapid computer-controlled UV lamp setting allows rapidly scanning UV lamp settings during an experiment, and has unique applications to OFR experiments in field studies (Hu et al., 2015; Ortega et al., 2015; Palm et al., 2016). In these experiments, OFRs enable the exploration of a very large range of photochemical age during a short period (~2 hr) when ambient conditions often do not significantly change.”**

R2.16) P23549, L21: subscript “exp” in “OHexp”.

We thank the Referee for pointing out this typo and have corrected it.

R2.17) P23550, L16: suggested revision: “estimate ~~some~~ **parameters that are not specified or measured** (e.g. UV) as needed”.

We have revised this sentence as suggested by the Referee.

R2.18) P23551, L3: “Photolysis of SOA, **a pathway ignored in previous OFR studies**, is also investigated.” SOA photolysis is considered in Lambe et al. (2013), which uses an OFR. Photolysis of  $\alpha$ -pinene SOA generated in a flow cell is characterized by Epstein et al. (2014), and photolysis of several SOA types generated in a flow cell were characterized by Romonosky et al. (2015).

We have removed the text bolded by the Referee. The sentence in P23551/L3 now reads:

**“Photolysis of SOA is also investigated.”**

R2.19) P23552, L24: Elsewhere in the manuscript, the “low” water vapor mixing ratio is represented as 0.07% rather than 0.0007.

We have changed “0.0007” here to “0.07%” to maintain consistency.

R2.20) P23558, L26: Replace “experimenter” with “experimentalist”.

We have made this change as suggested by the Referee.

R2.21) P23565, L7: Replace “faithfully” with “accurately”.

We have made this change as suggested by the Referee.

## References (for responses to both reviewers)

- Aimantant, S. and Ziemann, P. J.: Chemical Mechanisms of Aging of Aerosol Formed from the Reaction of n-Pentadecane with OH Radicals in the Presence of NO<sub>x</sub>, *Aerosol Sci. Technol.*, 47(9), 979–990, doi:10.1080/02786826.2013.804621, 2013.
- Alif, A., Pilichowski, J. and Boule, P.: photochemistry and environment XIII phototransformation of 2-nitrophenol in aqueous solution, *J. Photochem. Photobiol. A Chem.*, 59, 209–219, doi:10.1016/1010-6030(91)87009-K, 1991.
- Ammann, M., Cox, R. A., Crowley, J. N., Jenkin, M. E., Mellouki, A., Rossi, M. J., Troe, J., Wallington, T. J., Cox, B., Atkinson, R., Baulch, D. L. and Kerr, J. A.: IUPAC Task Group on Atmospheric Chemical Kinetic Data Evaluation, [online] Available from: <http://iupac.pole-ether.fr/#>, 2015.
- Atkinson, R. and Arey, J.: Atmospheric degradation of volatile organic compounds., *Chem. Rev.*, 103(12), 4605–38, doi:10.1021/cr0206420, 2003.
- Baulch, D. L., Bowman, C. T., Cobos, C. J., Cox, R. A., Just, T., Kerr, J. A., Pilling, M. J., Stocker, D., Troe, J., Tsang, W., Walker, R. W. and Warnatz, J.: Evaluated kinetic data for combustion modeling: Supplement II, *J. Phys. Chem. Ref. Data*, 34(3), 757–1397, doi:10.1063/1.1748524, 2005.
- Baulch, D. L., Cobos, C. J., Cox, R. A., Esser, C., Frank, P., Just, T., Kerr, J. A., Pilling, M. J., Troe, J., Walker, R. W. and Warnatz, J.: Evaluated Kinetic Data for Combustion Modelling, *J. Phys. Chem. Ref. Data*, 21(3), 411, doi:10.1063/1.555908, 1992.
- Bouzidi, H., Aslan, L., El Dib, G., Coddeville, P., Fittschen, C. and Tomas, A.: Investigation of the Gas-Phase Photolysis and Temperature-Dependent OH Reaction Kinetics of 4-Hydroxy-2-butanone, *Environ. Sci. Technol.*, 49(20), 12178–12186, doi:10.1021/acs.est.5b02721, 2015.
- Bouzidi, H., Laversin, H., Tomas, a., Coddeville, P., Fittschen, C., El Dib, G., Roth, E. and Chakir, a.: Reactivity of 3-hydroxy-3-methyl-2-butanone: Photolysis and OH reaction kinetics, *Atmos. Environ.*, 98(3), 540–548, doi:10.1016/j.atmosenv.2014.09.033, 2014.
- Burdett, J. L. and Rogers, M. T.: Keto-Enol Tautomerism in  $\beta$ -Dicarbonyls Studied by Nuclear Magnetic Resonance Spectroscopy. 1 I. Proton Chemical Shifts and Equilibrium Constants of Pure Compounds, *J. Am. Chem. Soc.*, 86(11), 2105–2109, doi:10.1021/ja01065a003, 1964.
- Calvert, J. G., Atkinson, R., Becker, K. H., Kamens, R. M., Seinfeld, J. H., Wallington, T. H. and Yarwood, G.: *The Mechanisms of Atmospheric Oxidation of the Aromatic Hydrocarbons*, Oxford University Press, USA. [online] Available from: <https://books.google.com/books?id=P0basaLrxDMC>, 2002.
- Carey, F. A. and Sundberg, R. J.: *Advanced Organic Chemistry. Part A: Structure and Mechanisms*, 5th ed., Springer US, Boston, MA., 2007.
- Cours, T., Canneaux, S. and Bohr, F.: Features of the potential energy surface for the reaction of HO<sub>2</sub> radical with acetone, *Int. J. Quantum Chem.*, 107(6), 1344–1354, doi:10.1002/qua.21269, 2007.
- Docherty, K. S., Wu, W., Lim, Y. Bin and Ziemann, P. J.: Contributions of Organic Peroxides to Secondary Aerosol Formed from Reactions of Monoterpenes with O<sub>3</sub>, *Environ. Sci. Technol.*, 39(11), 4049–4059, doi:10.1021/es050228s, 2005.
- Epstein, S. A., Blair, S. L. and Nizkorodov, S. A.: Direct Photolysis of  $\alpha$ -Pinene Ozonolysis Secondary Organic Aerosol: Effect on Particle Mass and Peroxide Content, *Environ. Sci.*

Technol., 48(19), 11251–8, doi:10.1021/es502350u, 2014.

Epstein, S. A., Shemesh, D., Tran, V. T., Nizkorodov, S. A. and Gerber, R. B.: Absorption Spectra and Photolysis of Methyl Peroxide in Liquid and Frozen Water, *J. Phys. Chem. A*, 116(24), 6068–6077, doi:10.1021/jp211304v, 2012.

Evans, R. C., Douglas, P. and Burrow, H. D., Eds.: *Applied Photochemistry*, Springer Netherlands, Dordrecht., 2013.

Foster, R.: *Organic Charge-Transfer Complexes*, Academic Press, New York., 1969.

Francisco, J. S. and Eisfeld, W.: Atmospheric Oxidation Mechanism of Hydroxymethyl Hydroperoxide †, *J. Phys. Chem. A*, 113(26), 7593–7600, doi:10.1021/jp901735z, 2009.

Gäb, S., Hellpointner, E., Turner, W. V. and Kofte, F.: Hydroxymethyl hydroperoxide and bis(hydroxymethyl) peroxide from gas-phase ozonolysis of naturally occurring alkenes, *Nature*, 316(6028), 535–536, doi:10.1038/316535a0, 1985.

Gao, H. and Zepp, R. G.: Factors Influencing Photoreactions of Dissolved Organic Matter in a Coastal River of the Southeastern United States, *Environ. Sci. Technol.*, 32(19), 2940–2946, doi:10.1021/es9803660, 1998.

Gierczak, T. and Ravishankara, A. R.: Does the HO<sub>2</sub> radical react with ketones?, *Int. J. Chem. Kinet.*, 32(9), 573–580, doi:10.1002/1097-4601(2000)32:9<573::AID-KIN7>3.0.CO;2-V, 2000.

Goldstein, S., Aschengrau, D., Diamant, Y. and Rabani, J.: Photolysis of Aqueous H<sub>2</sub>O<sub>2</sub>: Quantum Yield and Applications for Polychromatic UV Actinometry in Photoreactors, *Environ. Sci. Technol.*, 41(21), 7486–7490, doi:10.1021/es071379t, 2007.

Hodzic, A., Madronich, S., Kasibhatla, P. S., Tyndall, G., Aumont, B., Jimenez, J. L., Lee-Taylor, J. and Orlando, J.: Organic photolysis reactions in tropospheric aerosols: effect on secondary organic aerosol formation and lifetime, *Atmos. Chem. Phys.*, 15(16), 9253–9269, doi:10.5194/acp-15-9253-2015, 2015.

Hu, W. W., Campuzano-Jost, P., Palm, B. B., Day, D. A., Ortega, A. M., Hayes, P. L., Krechmer, J. E., Chen, Q., Kuwata, M., Liu, Y. J., de Sá, S. S., McKinney, K., Martin, S. T., Hu, M., Budisulistiorini, S. H., Riva, M., Surratt, J. D., St. Clair, J. M., Isaacman-Van Wertz, G., Yee, L. D., Goldstein, A. H., Carbone, S., Brito, J., Artaxo, P., de Gouw, J. A., Koss, A., Wisthaler, A., Mikoviny, T., Karl, T., Kaser, L., Jud, W., Hansel, A., Docherty, K. S., Alexander, M. L., Robinson, N. H., Coe, H., Allan, J. D., Canagaratna, M. R., Paulot, F. and Jimenez, J. L.: Characterization of a real-time tracer for isoprene epoxydiols-derived secondary organic aerosol (IEPOX-SOA) from aerosol mass spectrometer measurements, *Atmos. Chem. Phys.*, 15(20), 11807–11833, doi:10.5194/acp-15-11807-2015, 2015.

Johannessen, S. C. and Miller, W. L.: Quantum yield for the photochemical production of dissolved inorganic carbon in seawater, *Mar. Chem.*, 76(4), 271–283, doi:10.1016/S0304-4203(01)00067-6, 2001.

Kang, E., Toohey, D. W. and Brune, W. H.: Dependence of SOA oxidation on organic aerosol mass concentration and OH exposure: experimental PAM chamber studies, *Atmos. Chem. Phys.*, 11(4), 1837–1852, doi:10.5194/acp-11-1837-2011, 2011.

Keller-Rudek, H., Moortgat, G. K., Sander, R. and Sörensen, R.: *The MPI-Mainz UV/VIS Spectral Atlas of Gaseous Molecules of Atmospheric Interest*, [online] Available from: [www.uv-vis-spectral-atlas-mainz.org](http://www.uv-vis-spectral-atlas-mainz.org), 2015.

Klems, J. P., Lipka, K. a and McGivern, W. S.: *Quantitative Evidence for Organic Peroxy*

Radical Photochemistry at 254 nm, *J. Phys. Chem. A*, 119(2), 344–351, doi:10.1021/jp509165x, 2015.

Kumar, M. and Francisco, J. S.: Red-Light-Induced Decomposition of an Organic Peroxy Radical: A New Source of the HO<sub>2</sub> Radical, *Angew. Chemie Int. Ed.*, doi:10.1002/anie.201509311, 2015.

Kwok, E. and Atkinson, R.: Estimation of hydroxyl radical reaction rate constants for gas-phase organic compounds using a structure-reactivity relationship: An update, *Atmos. Environ.*, 29(14), 1685–1695, doi:10.1016/1352-2310(95)00069-B, 1995.

Lambe, A. T., Cappa, C. D., Massoli, P., Onasch, T. B., Forestieri, S. D., Martin, A. T., Cummings, M. J., Croasdale, D. R., Brune, W. H., Worsnop, D. R. and Davidovits, P.: Relationship between Oxidation Level and Optical Properties of Secondary Organic Aerosol, *Environ. Sci. Technol.*, 47(12), 6349–6357, doi:10.1021/es401043j, 2013.

Lambe, A. T., Onasch, T. B., Massoli, P., Croasdale, D. R., Wright, J. P., Ahern, A. T., Williams, L. R., Worsnop, D. R., Brune, W. H. and Davidovits, P.: Laboratory studies of the chemical composition and cloud condensation nuclei (CCN) activity of secondary organic aerosol (SOA) and oxidized primary organic aerosol (OPOA), *Atmos. Chem. Phys.*, 11(17), 8913–8928, doi:10.5194/acp-11-8913-2011, 2011.

Laue, T. and Plagens, A.: *Named Organic Reactions*, 2nd ed., John Wiley & Sons, Chichester, England, New York. [online] Available from: <http://www.wiley.com/WileyCDA/WileyTitle/productCd-047001041X.html>, 2005.

Li, R., Palm, B. B., Ortega, A. M., Hu, W., Peng, Z., Day, D. A., Knote, C., Brune, W. H., de Gouw, J. and Jimenez, J. L.: Modeling the radical chemistry in an Oxidation Flow Reactor (OFR): radical formation and recycling, sensitivities, and OH exposure estimation equation, *J. Phys. Chem. A*, 119(19), 4418–4432, doi:10.1021/jp509534k, 2015.

Liu, P. F., Abdelmalki, N., Hung, H.-M., Wang, Y., Brune, W. H. and Martin, S. T.: Ultraviolet and visible complex refractive indices of secondary organic material produced by photooxidation of the aromatic compounds toluene and m-Xylene, *Atmos. Chem. Phys.*, 15(3), 1435–1446, doi:10.5194/acp-15-1435-2015, 2015.

Liu, P., Zhang, Y. and Martin, S. T.: Complex refractive indices of thin films of secondary organic materials by spectroscopic ellipsometry from 220 to 1200 nm, *Environ. Sci. Technol.*, 47, 13594–13601, doi:10.1021/es403411e, 2013.

Messaadia, L., El Dib, G., Ferhati, A. and Chakir, A.: UV–visible spectra and gas-phase rate coefficients for the reaction of 2,3-pentanedione and 2,4-pentanedione with OH radicals, *Chem. Phys. Lett.*, 626, 73–79, doi:10.1016/j.cplett.2015.02.032, 2015.

O’Sullivan, D. W., Neale, P. J., Coffin, R. B., Boyd, T. J. and Osburn, C. L.: Photochemical production of hydrogen peroxide and methylhydroperoxide in coastal waters, *Mar. Chem.*, 97(1-2), 14–33, doi:10.1016/j.marchem.2005.04.003, 2005.

Ortega, A. M., Day, D. A., Cubison, M. J., Brune, W. H., Bon, D., de Gouw, J. A. and Jimenez, J. L.: Secondary organic aerosol formation and primary organic aerosol oxidation from biomass-burning smoke in a flow reactor during FLAME-3, *Atmos. Chem. Phys.*, 13(22), 11551–11571, doi:10.5194/acp-13-11551-2013, 2013.

Ortega, A. M., Hayes, P. L., Peng, Z., Palm, B. B., Hu, W., Day, D. A., Li, R., Cubison, M. J., Brune, W. H., Graus, M., Warneke, C., Gilman, J. B., Kuster, W. C., de Gouw, J. A. and Jimenez, J. L.: Real-time measurements of secondary organic aerosol formation and aging from

ambient air in an oxidation flow reactor in the Los Angeles area, *Atmos. Chem. Phys. Discuss.*, 15(15), 21907–21958, doi:10.5194/acpd-15-21907-2015, 2015.

Osburn, C. L., Retamal, L. and Vincent, W. F.: Photoreactivity of chromophoric dissolved organic matter transported by the Mackenzie River to the Beaufort Sea, *Mar. Chem.*, 115(1-2), 10–20, doi:10.1016/j.marchem.2009.05.003, 2009.

Palm, B. B., Campuzano-Jost, P., Ortega, A. M., Day, D. A., Kaser, L., Jud, W., Karl, T., Hansel, A., Hunter, J. F., Cross, E. S., Kroll, J. H., Peng, Z., Brune, W. H. and Jimenez, J. L.: In situ secondary organic aerosol formation from ambient pine forest air using an oxidation flow reactor, *Atmos. Chem. Phys.*, 16(5), 2943–2970, doi:10.5194/acp-16-2943-2016, 2016.

Peng, Z., Day, D. A., Stark, H., Li, R., Lee-Taylor, J., Palm, B. B., Brune, W. H. and Jimenez, J. L.: HOx radical chemistry in oxidation flow reactors with low-pressure mercury lamps systematically examined by modeling, *Atmos. Meas. Tech.*, 8(11), 4863–4890, doi:10.5194/amt-8-4863-2015, 2015.

Phillips, S. M. and Smith, G. D.: Light Absorption by Charge Transfer Complexes in Brown Carbon Aerosols, *Environ. Sci. Technol. Lett.*, 1(10), 382–386, doi:10.1021/ez500263j, 2014.

Phillips, S. M. and Smith, G. D.: Further Evidence for Charge Transfer Complexes in Brown Carbon Aerosols from Excitation–Emission Matrix Fluorescence Spectroscopy, *J. Phys. Chem. A*, 119(19), 4545–4551, doi:10.1021/jp510709e, 2015.

Pitts, J. N. and Finlayson, B. J.: Mechanismen der photochemischen Luftverschmutzung, *Angew. Chemie*, 87(1), 18–33, doi:10.1002/ange.19750870103, 1975.

Pretsch, E., Bühlmann, P. and Badertscher, M.: Structure Determination of Organic Compounds, Springer Berlin Heidelberg, Berlin, Heidelberg., 2009.

Romonosky, D. E., Ali, N. N., Saiduddin, M. N., Wu, M., Lee, H. J. (Julie), Aiona, P. K. and Nizkorodov, S. A.: Effective absorption cross sections and photolysis rates of anthropogenic and biogenic secondary organic aerosols, *Atmos. Environ.*, 130, 172–179, doi:10.1016/j.atmosenv.2015.10.019, 2016.

Sharpless, C. M. and Blough, N. V.: The importance of charge-transfer interactions in determining chromophoric dissolved organic matter (CDOM) optical and photochemical properties, *Environ. Sci. Process. Impacts*, 16(4), 654, doi:10.1039/c3em00573a, 2014.

da Silva, G. and Bozzelli, J. W.: Role of the  $\alpha$ -hydroxyethylperoxy radical in the reactions of acetaldehyde and vinyl alcohol with HO<sub>2</sub>, *Chem. Phys. Lett.*, 483(1-3), 25–29, doi:10.1016/j.cplett.2009.10.045, 2009.

Strollo, C. M. and Ziemann, P. J.: Products and mechanism of secondary organic aerosol formation from the reaction of 3-methylfuran with OH radicals in the presence of NO<sub>x</sub>, *Atmos. Environ.*, 77, 534–543, doi:10.1016/j.atmosenv.2013.05.033, 2013.

Tkacik, D. S., Lambe, A. T., Jathar, S., Li, X., Presto, A. A., Zhao, Y., Blake, D., Meinardi, S., Jayne, J. T., Croteau, P. L. and Robinson, A. L.: Secondary Organic Aerosol Formation from in-Use Motor Vehicle Emissions Using a Potential Aerosol Mass Reactor, *Environ. Sci. Technol.*, 48(19), 11235–11242, doi:10.1021/es502239v, 2014.

Tsang, W.: Chemical kinetic data base for combustion chemistry part V. Propene, *J. Phys. Chem. Ref. data*, 20(2), 221–274, doi:10.1063/1.555880, 1991.

Turro, N. J., Ramamurthy, V. and Scaiano, J. C.: Principles of Molecular Photochemistry: An Introduction, University Science Books, Sausalito, CA, USA. [online] Available from:

<http://www.uscibooks.com/turro2.htm>, 2009.

Updyke, K. M., Nguyen, T. B. and Nizkorodov, S. a.: Formation of brown carbon via reactions of ammonia with secondary organic aerosols from biogenic and anthropogenic precursors, *Atmos. Environ.*, 63, 22–31, doi:10.1016/j.atmosenv.2012.09.012, 2012.

Wolfe, G. M., Crouse, J. D., Parrish, J. D., St. Clair, J. M., Beaver, M. R., Paulot, F., Yoon, T. P., Wennberg, P. O. and Keutsch, F. N.: Photolysis, OH reactivity and ozone reactivity of a proxy for isoprene-derived hydroperoxyenals (HPALDs), *Phys. Chem. Chem. Phys.*, 14(20), 7276, doi:10.1039/c2cp40388a, 2012.

Wong, J. P. S., Zhou, S. and Abbatt, J. P. D.: Changes in Secondary Organic Aerosol Composition and Mass due to Photolysis: Relative Humidity Dependence, *J. Phys. Chem. A*, 119(19), 4309–4316, doi:10.1021/jp506898c, 2015.

Zhang, Y., Xie, H. and Chen, G.: Factors Affecting the Efficiency of Carbon Monoxide Photoproduction in the St. Lawrence Estuarine System (Canada), *Environ. Sci. Technol.*, 40(24), 7771–7777, doi:10.1021/es0615268, 2006.

Ziemann, P. and Atkinson, R.: Kinetics, products, and mechanisms of secondary organic aerosol formation, *Chem. Soc. Rev.*, 41(19), 6582, doi:10.1039/c2cs35122f, 2012.